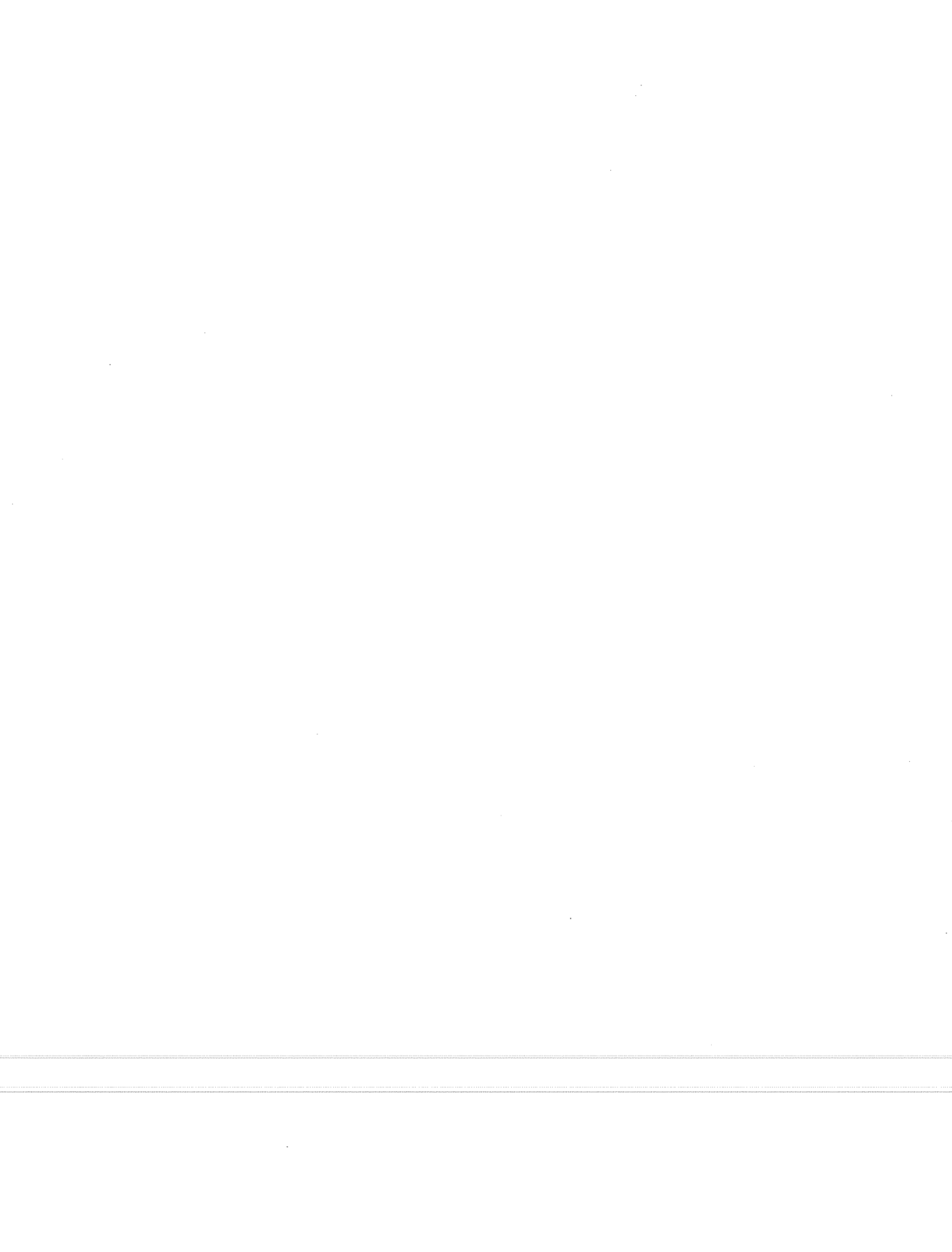# EFFECTS OF BAR DEFORMATION AND CONCRETE STRENGTH ON

BOND ON REINFORCING STEEL TO CONCRETE
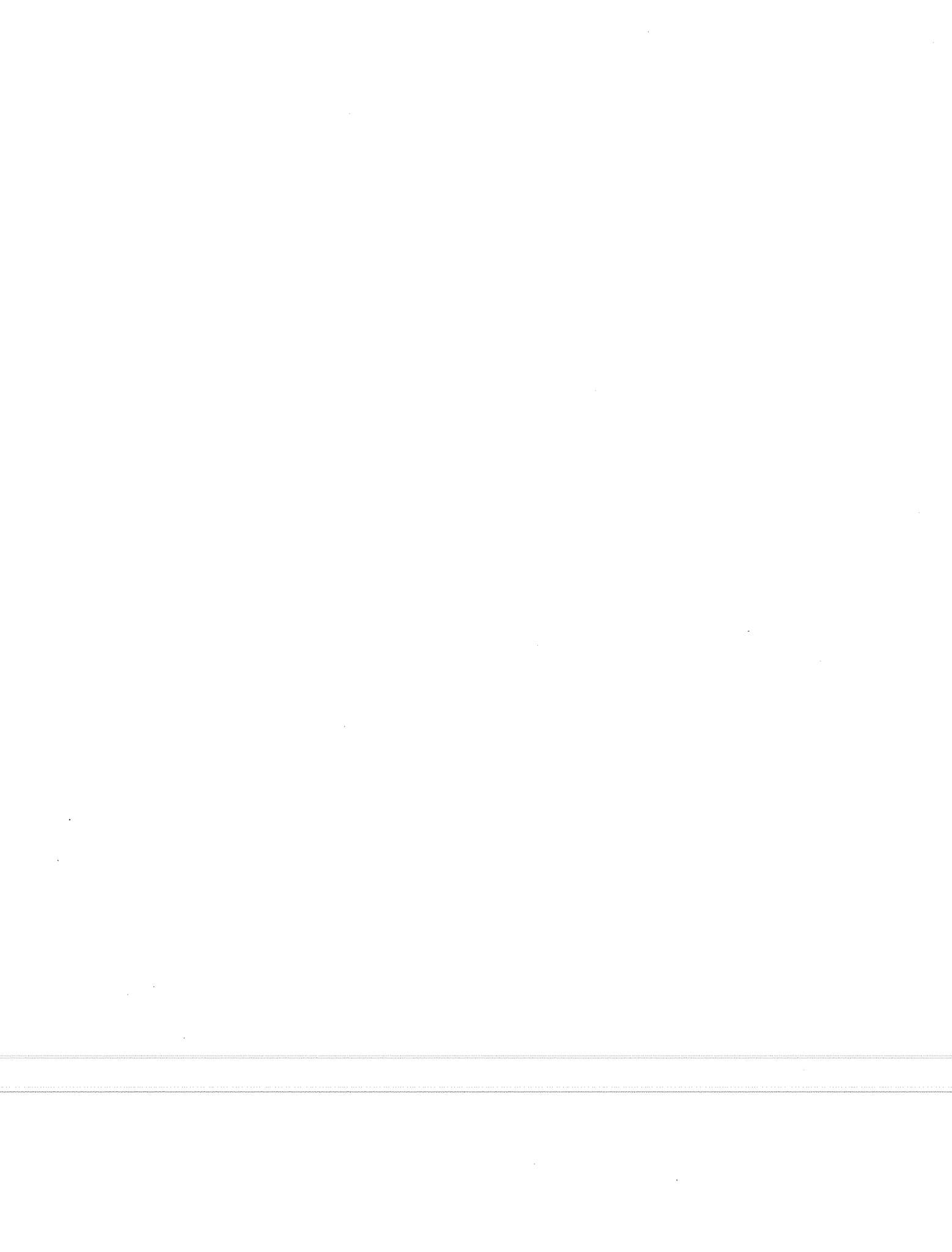
by

Hideki Kimura

James O. Jirsa

ABSTRACT

Current ASTM deformation requirements for reinforcement are based on research conducted over 30 years ago. Since that time increases in steel and concrete strengths have resulted in a trend to design smaller and more congested structural members. Concrete strengths used today are two to three times greater than those in use when the current deformed bars were developed. The objective of this study is

(1)   to seek improvements in deformed bar geometries which could reduce development length, and

(2)   to provide technical data on bond between high strength concrete and reinforcing steel.

Existing data, especially recent work done in Japan, is reviewed prior to selecting deformation geometry (rib height, rib face angle and rib spacing).

ACKNOWLEDGEMENTS

TABLE OF CONTENTS

LIST OF FIGURES

LIST OF TABLES
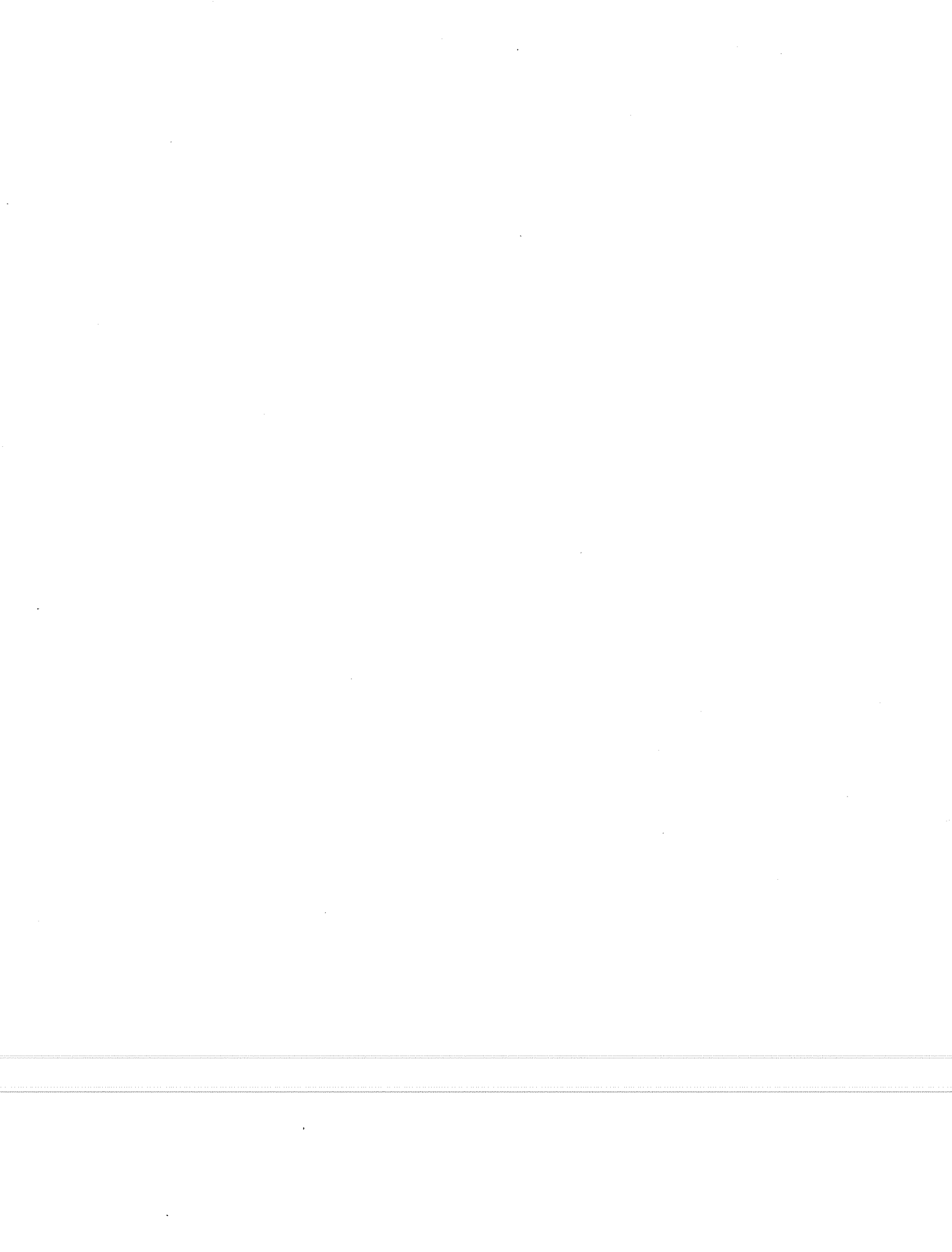
LIST OF PHOTOS

CHAPTER 1

Introduction

Current ASTM deformation requirements for reinforcing bar are based on research conducted over 30 years ago. Since that time increases in steel and concrete strengths have resulted in a trend to design smaller and more congested structural members. Concrete strengths used today are two to three times greater than those in use when the current deformed bars were developed. In such members, closely-spaced bars are placed near the surface and the cover is likely to split if anchorage distress or failure occurs. Therefore, splitting of the concrete surrounding the reinforcement is a major issue.

The objective of this study is to seek improvements of deformed bar geometries which could reduce development length and to provide technical data on bond between high strength concrete and reinforcing steel.

There is a considerable body of existing research on bar deformation patterns and geometry. The intent is to utilize fully the existing data to select deformation geometry, particularly rib height, rib face angle and rib spacing. Special attention is directed to recent work in Japan which has not yet been translated or has appeared in English literature. In a real structure, splitting may be the dominant mode of failure. The intent of this study is to simulate the conditions around an anchored reinforcing bar.
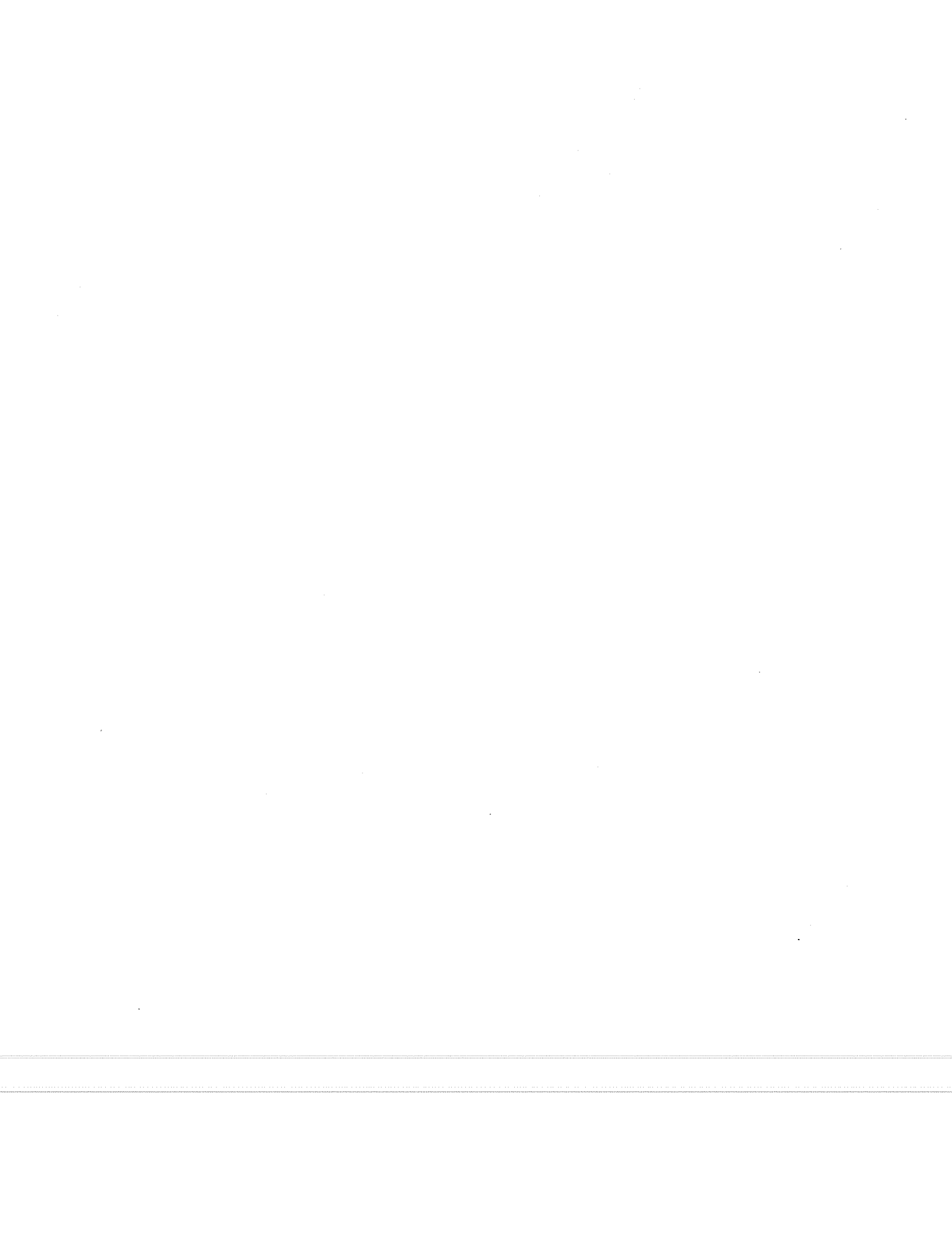
CHAPTER 2

Previous research on the role of bar geometry on bond

Considerable research which focus on the effect of bar deformation on bond between steel reinforcing bars and surrounding concrete have been performed. Most of these studies have had an empirical emphasis. The following literature survey briefly outlines that research work. Previous research, except that done in Japan, is introduced in Sec. 2.1. In Sec. 2.2, special attention is paid to recent studies in Japan which have not yet been translated or have appeared in English literature.

2.1 Outline of previous research conducted outside of Japan

Research on the effect of deformations on bond goes back at least as far as 1913, when Abrams reported tests of bond between steel and concrete [1]. The pullout test results indicated that the ribs had little effect up to an end slip of 0.010 in., after which the ribs became effective in taking bond stress. He suggested that if high bond resistance was desired, the rib height should be 1/10 of the bar diameter and spaced 1/2 bar diameter apart. Also the plane of the bearing faces of the ribs should be as close as possible to 90 degrees from the longitudinal axis of the bar.

Menzel, in 1939, examined the influence of the bearing area on bond [2]. His report showed that bars with longitudinal ribs had smaller stiffness and smaller ultimate bond strength than bars with transverse ribs. Rib face angles from 45 to 57 degrees did not show a significant difference in bond - slip behavior.

Clark, in 1946, performed 204 pullout tests on 17 different deformed bar patterns [3,4]. He found that the pattern of deformations did not seem to be an important factor in determining the bond resistance, but the greater the bearing rib angle, the better was the bond resistance. A maximum ratio of the shearing to bearing areas of 5 or 6 was desirable for good bond behavior if the requirements of ASTM A305 were met. ASTM A305 specifications for bar deformations are credited to Clark's work.

Rehm, in 1957, studied geometrical properties of ribs using single rib bars with a short bonded length of one bar diameter [5].

3

He found that for equal rib bearing stress the slip was proportional to the rib height when the rib height was less than 2 mm. The rate of increase of slip with rib height became less for the rib height greater than 2 mm.

In 1963, Shah performed static and dynamic tests on concrete shear keys [6]. It was found that the number of shear keys played the most important roll on shear strength. The total strength of concrete shear keys did not increase in proportion to their numbers; with the increase in shear keys, the average shear strength decreased. A similar effect was observed in dynamic tests. The reason for this decrease in unit strength with increase in number of keys was due to a progressive failure of keys. Most of the load was initially carried by the first row of keys, and the second and third rows of keys only carried load as the system deformed. Since only small deformations could develop before failure occurred it was not possible for all keys to simultaneously carry their maximum load capacities, and a progressive failure resulted.

The effect of rib height on bond was examined by Ferguson in 1965 [7]. Two groups of specimens were made for pullout tests. One group had full-height ribs and the other had ribs which were 10 % deficient in height. There was no significant difference in the loaded end slips up to 0.01 in., although it appeared that at large slips, the full-height rib performed better. The ultimate bond stress for the full-height rib was 10 to 15 % lower than that of the deficient rib.

Lutz and Gergely (1967, 1970) performed a modified pullout test to study the effect of the bar surface geometry on bond [8]. Bars with rib face angles larger than 45 degrees slipped mainly by compression and crushing of concrete in front of the ribs, on the other hand, bars with rib face angles smaller than 45 degrees slipped mainly by a sliding movement. Eccentric pullout tests showed that bars with smaller rib spacing and higher ribs performed better in bond. Considerable improvement in the free end slip characteristics, and lesser but still significant increases (15 to 20 %) of the ultimate strength were observed.

Wilhelm, Kemp, and Lee, in 1971, reported that as long as bars met ASTM A305 specifications, the various manufacturer's patterns produced almost the same bond behavior [9].

Skorobogatov and Edwards, in 1979, studied the effect of rib face angle [10]. They reported that rib face angles of 48.5 and

57.8 degrees did not show significant differences in maximum bond stress because the bar with larger face angle was modified by crushed concrete wedges (truncated cones) in the rib fillet which effectively reduced the rib angle to a smaller value. They suggested that more research is not required to study the effect of rib angle on the bond strength.

In Sweden, Losberg and Olsson (1979) conducted three types of bond tests; pullout tests, beam end tests and ring pullout tests [11]. They showed that there was little influence of rib spacing on bond strength. Rib spacings used in Sweden are unnecessarily small. They also reported that the rib height had much less influence than that would have been indicated by pullout tests.

Soretz and Hölzenbein (1979) in Germany performed pullout test to investigate the effect of bar geometry [12]. They suggested a minimum rib height of 0.03 diameter for delaying the onset of splitting. As rib height is reduced, rib spacing must be reduced appropriately. They reported that the variation of rib angle with respect to bar axis from 45 to 90 degrees improved bond performance slightly. They also found that the rib face angles of 45 to 90 degrees did not show a significant influence on bond performance.

2.2 Summary of recent studies in Japan

In the 1970's, the need to use large-diameter deformed bars for large size structures, such as nuclear power plants, foundations of long span bridges and mats for underground oil tank resulted in many research projects on D51 deformed bars (diameter of 51 mm) in Japan. Those projects involved experimental studies on bar geometry, anchorage, splices, bendability, weldability and fatigue properties. Results of the research are summarized in "Design Guideline of Reinforced Concrete Structures Using Large Size Deformed Bars" published by Japanese Society of Civil Engineering (JSCE) in August, 1977. Today, it is possible to produce even larger size threaded reinforcing bars such as D57, D64 and D70. "Recommendations for Design and Construction of Reinforced Concrete Structures Using Large Size D57 and D64 Threaded Reinforcing Bars" was also issued by JSCE in 1992. In this section, the effects of bar deformation and concrete strength on bond of reinforcing steel to concrete are emphasized.

1] Murata,J. and Kawai,A., "Studies on Bond Strength of Deformed Bar by Pull-Out Test", Journal of Japanese Society of Civil Engineering, No.348/v-1, August 1984, pp.113-122.(in Japanese)

Murata and Kawai performed two types of pull-out tests on bond strength of deformed bars. The splitting pull-out test was proposed to evaluate not only the splitting bond strength but also the initial bond strength, which gave information about adhesion between the steel bar and concrete. For pullout failures, eccentric pull-out tests were conducted to estimate the ultimate bond strength. Specimens are shown in Fig.2.1. Test specimens were produced by machining plain bars and modifying deformed bars (D32: 32 mm dia.) to obtain varying rib spacing ($0.5d_b$ - $3.0d_b$), rib height (1.0, 1.5, 2.0 and 2.5mm), and rib face angles (15 to 90 degrees in 5 degrees increments). They also investigated bond characteristics of 5 different kinds of commercial deformed bars of varying diameters (D16-D57 : #5-#18).

The following conclusions were made:

1) The splitting bond strength increased with the rib face angle up to 45° and showed constant values for rib face angles of 45° or more. Rib face angles greater than 45° were recommended for the deformed bars.(Fig.2.2)

2) The splitting bond strength was approximately constant when the rib spacing was less than the bar diameter, but decreased when spacings greater than one bar diameter were used (Fig.2.3). The splitting bond strength increased almost linearly with the rib height for rib heights up to 8 % of the bar diameter (Fig.2.4).

3) The ultimate bond strength increased in proportion to the rib spacing up to $2.5d_b$. The bars with rib spacing of $2.5d_b$ had a 20% increase in ultimate bond strength compared with spacing of $0.5d_b$ (Fig.2.5). The ultimate bond strength increased slightly (10%) as the rib height ranged from 2 to 8 % of the bar diameter (Fig.2.6). From 2) and 3), it was recommended that the proper rib spacing should be taken as the bar diameter or less, and the rib height from 7 % to 8 % of the bar diameter, respectively.

4) The concrete strength had a significant effect on splitting bond strength but only a very small effect on ultimate bond strength. (Note : The range of concrete strength used was low ; 19.6 to 39.2 MPa)

5) Bond characteristics of deformed bars with same deformation patterns (parallel or crescent etc.) would be the same for bars with different bar diameter provided that the bar dimension were the same ratio to the bar diameters.

6) The commercial bar with parallel deformations had larger initial bond strength and smaller displacements at splitting failure than those observed for a bar crescent shaped deformations. The rib spacing for both bars were 70 % of the bar diameter or less, so splitting bond strengths were almost the same but ultimate bond strength increased with rib spacing and rib height.

7) In the commercially produced deformed bar, the initial bond strength varied from 4.9 to 9.0 MPa according to the deformation pattern but the splitting bond strength was nearly constant with values from 11.8 to 12.7 MPa (except for some large bar sizes). The ultimate bond strengths ranged from 6.2 to 8.8 MPa depending on the rib spacing and rib height.
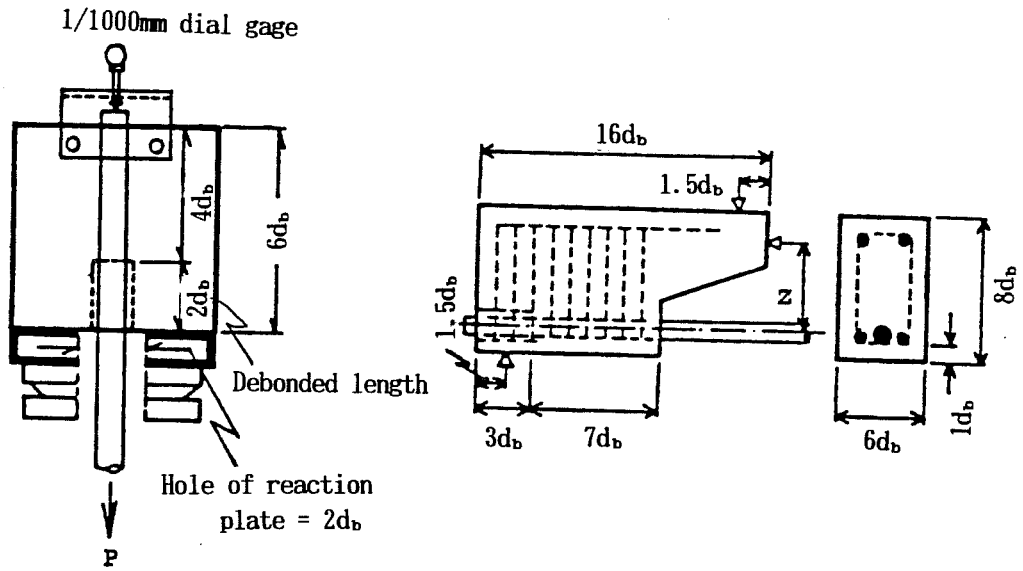
(a) Splitting pullout test specimen

(b) Eccentric pullout test specimen

Figure 2.1 Details of Specimens
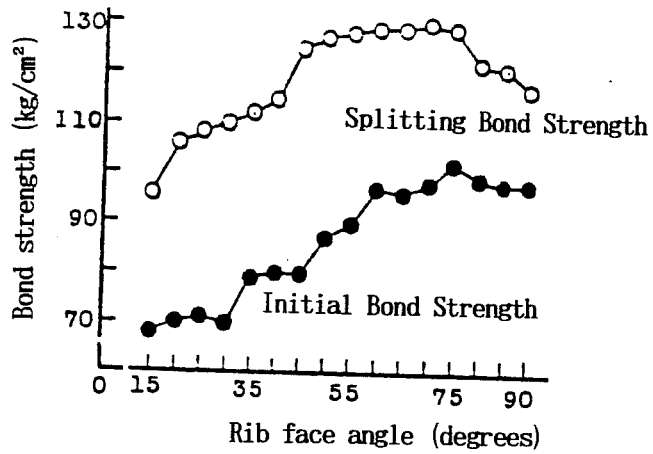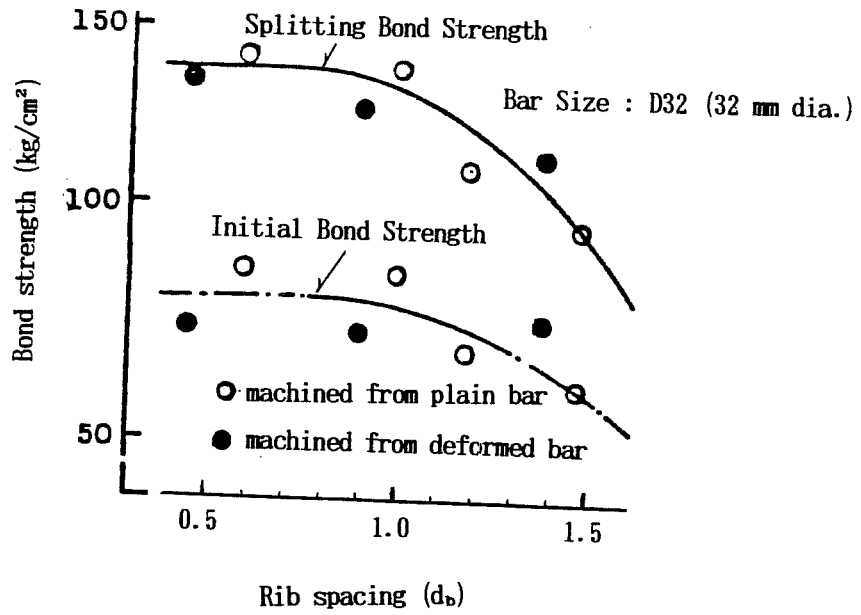

Figure 2.2 Effect of rib face angle

9

Figure 2.3 Effect of rib spacing

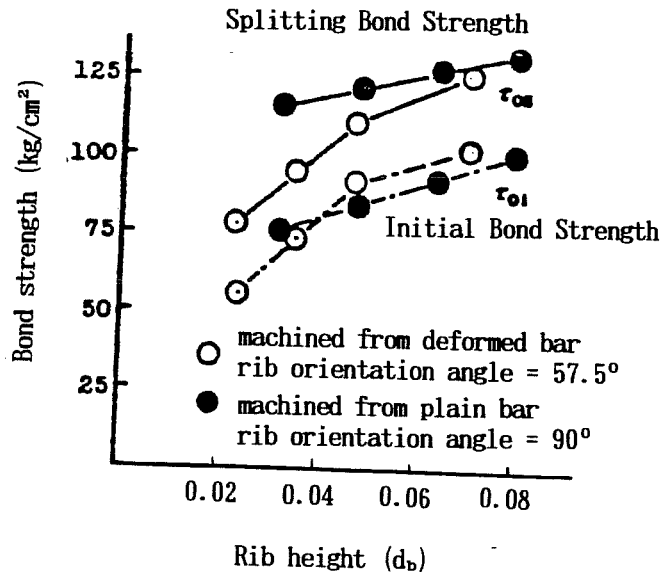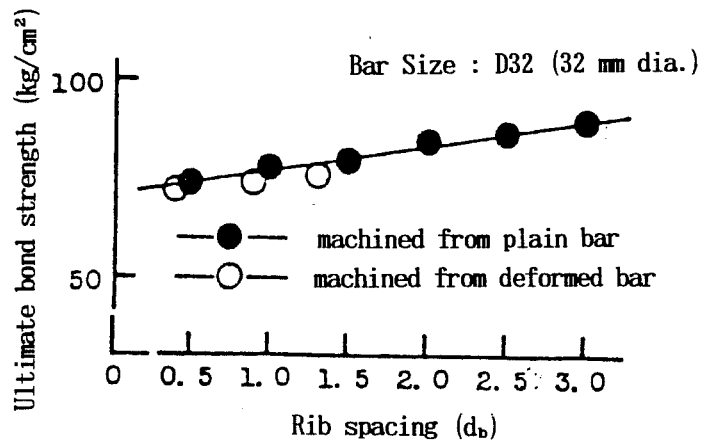
Figure 2.4 Effect of rib height

Figure 2.5 Effect of rib spacing on
ultimate bond strength
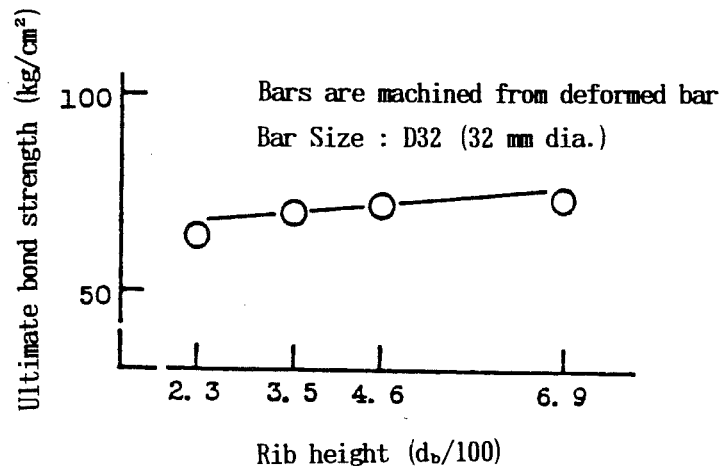
Figure 2.6 Effect of rib height on
ultimate bond strength

11

2] Kokubu, M. and Okamura, H., "Studies on Usage of Large Deformed Bar",Concrete Library No.43, Japanese Society of Civil Engineering, August 1977, pp.19-29 (in Japanese)

Kokubu and Okamura conducted pullout tests of D51(51mm dia.) bars made of cast iron. Twenty four different deformation patterns shown in Fig.2.7 were used. The bars were pulled from 250 mm cubes which were reinforced with 200 mm diameter spiral hoops spaced at 40 mm using 6 mm diameter steel bar. Compressive strength of concrete was 34.3 MPa when the test was conducted. The deformation patterns for D51 bars that exhibited relatively good bond performance were chosen for bending and fatigue tests of beams and the characteristics of cracking and fatigue resistance were investigated. The test results indicated that:

1) The effect of rib orientation angle (see Fig.2.8) was very small within a range from 46 to 90 degrees. Also the effect of rib face angle was small when the angle was 45 degrees or more (Fig.2.9). These factors were not taken into account in determining a bearing area coefficient (BA*).

2) Bond characteristics between deformed bars and surrounding concrete were affected primarily by three factors : rib height, rib spacing and rib projection length. It was shown that a bearing area coefficient (BA*) which included all three factors described bond characteristics very well as shown in Fig.2.10. BA* was given as follows.

$$BA^* = \frac{(\text{rib height}^{**}) \times (\text{rib projection length})}{(\text{rib spacing}) \times (\text{nominal perimeter})}$$

** : not greater than 0.2 rib spacing

A BA* of more than 0.1 is needed for large deformed bars. Bond strength increased as rib clear spacing decreased and as rib height increased. But if the ratio of rib height to rib clear spacing is too large, the shear capacity of concrete between ribs will decline because of a decrease in the interlocking effect of aggregate. Bond performance for such bars will

deteriorate. Therefore, an effective rib height for a given rib clear spacing was defined. For large deformed bars, the effective rib height was 20 % of the rib clear spacing.

3) Crack widths in R/C beams using large deformed bars which produced good bond performance in pullout tests, hardly increased during repeated loading. The residual crack widths under no load for specimens with large deformed bars were almost the same as those with 25 mm bars. The effects of bar arrangement, including effective concrete area per bar, and concrete cover on the crack width were larger than that of the bar size. Excessive crack widths should not be a problem under typical working stress conditions, provided that the large deformed bars have an appropriate bar deformation pattern with large BA* value and that the bars are properly arranged.

4) Generally, bars with rounded intersections between the ribs and the bar have better fatigue life because the stress concentrations are reduced. However, all large deformed bars showed less fatigue resistance than normal deformed bars. The deformation pattern for large deformed bars used in severe repeated loading conditions will need to be carefully considered.
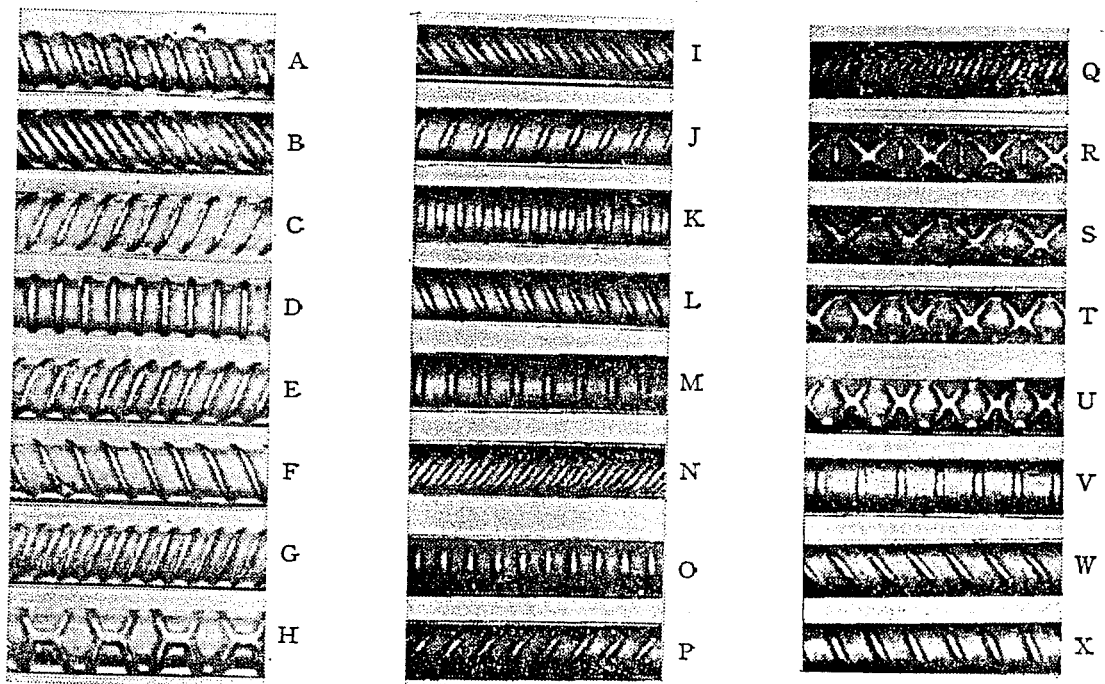
Figure 2.7 Deformation patterns of bars
for pullout test

$\left(\begin{array}{l} \tau_{0.1}, \quad \tau_{0.25} \text{ and } \quad \tau_{0.5} \quad \text{are bond stresses at 0.1, 0.25 and 0.5 mm slip.} \\ \tau_{max} \quad \text{is the maximun bond strength.} \end{array}\right)$
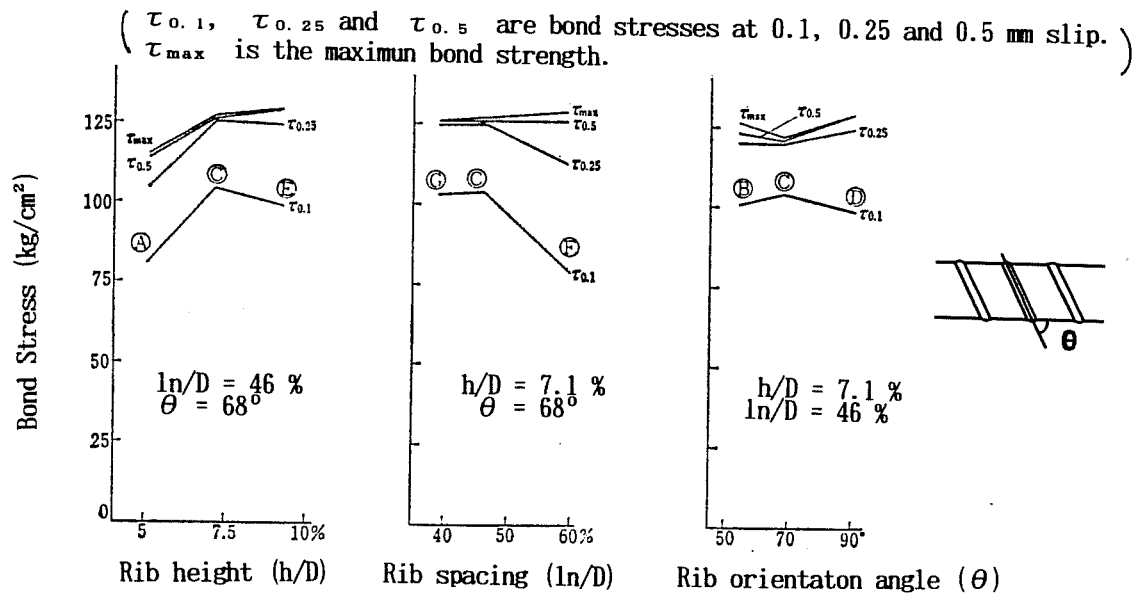
Figure 2.8 Effect of deformation factors on
bond characteristics

$\tau_{0.1}$, $\tau_{0.25}$ and $\tau_{0.5}$ are bond stresses at 0.1, 0.25 and 0.5 mm slip.

Figure 2.9 Effect of rib face angle
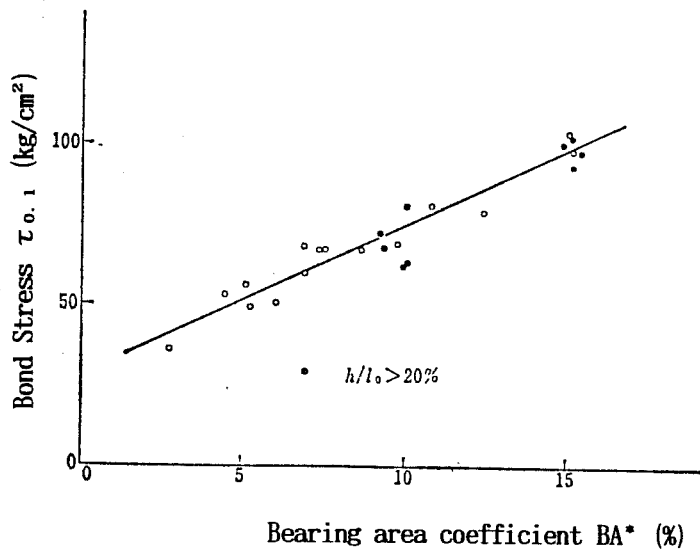
Figure 2.10 Relationship between BA* and bond stress
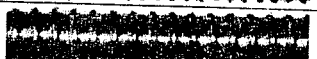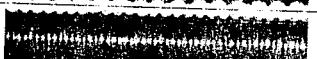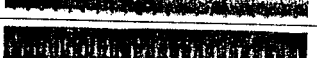
3]Goto,Y.,Shima,H. and Otsuka,K.,"Studies on Bond Characteristics of Large Deformed Bar",Concrete Library No.43,Japanese Society of Civil Engineering, August 1977, pp.43-54 (in Japanese)

To develop an appropriate bar deformation pattern for large size deformed bars, Goto addressed four issues related to bond characteristics : ① lateral crack (primary crack) patterns, ② internal crack (secondary crack) patterns, ③ bond stress-slip curves and ④ lap splices. The study consisted of four tests using two sizes, D41 and D51 (41 mm and 51 mm dia.), parallel deformed bars varying the lug height and the lug spacing as shown in Table 2.1. The bars were made by machining and by trial rolling. Concrete with compressive strength of 29.4 MPa was used. The results were summarized as follows.

1) Dispersion of lateral cracks (primary cracks) was evaluated using crack spacing. The maximum crack spacing (L_{max}) decreased as the lug spacing decreased (Fig.2.11) and lug height increased (Fig.2.12).
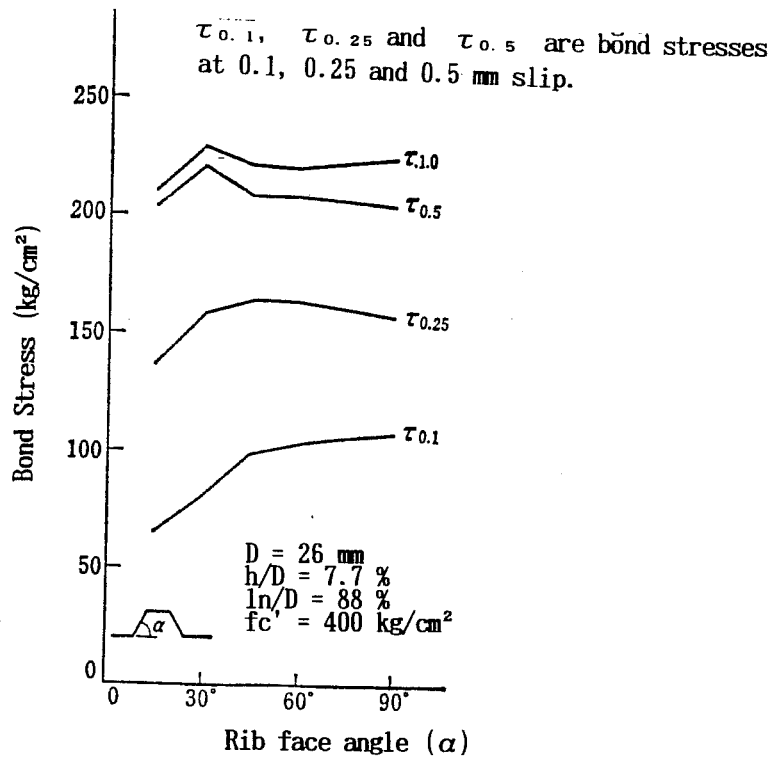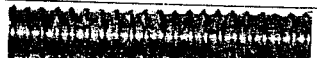
2) Goto photographed some specimens under tension, in which ink had been injected into the cracks in the concrete through a small longitudinal hole near the reinforcing bar. The equipment is shown in Fig.2.13. Figure 2.14 shows examples of internal cracks of D41 rolled bars, D51 machined bars and D51 rolled bars. The internal crack (secondary crack) started from the lug tips at an angle of approximately 60 degrees with the bar axis. In general, when the lug spacing was small, the number of the secondary cracks were large and those lengths were short. Therefore, the stress transfer from deformed bar to concrete was uniform as the lug spacing decreased and was a favorable pattern for improving the fatigue characteristics of the bar.

3) Using eccentric pullout tests, the relationships between bond stress and slip were examined. It was found that bars with small lug spacing had larger bond stresses at small slips than those with large lug spacing, although the differences was small at large slips.

4) Lap splices of large deformed bars would perform satisfactorily

provided that the lap length, cover thickness and confining reinforcement in the splice region are taken into account.

Table 2.1 Deformation patterns of bars for tests

Nominal diameter (mm)	Type of bar		Dimension of lug			Cross sectional area (cm²)	Surface deformation
			Spacing (mm)	Height (mm)	Width (mm)		
41	Rolled bar (Lateral lug)	Q	12	3.0	3.2	12.84	
		R	16	3.4	2.8	12.94	
		S	27	3.2	5.2	13.36	
51	Machining bar (Lateral lug)	A	15	4.5	2.5	18.80	
		B	20	4.5	3.0	20.03	
		C	12	3.5	2.5	19.22	
		D	15	3.5	2.5	20.10	
		E	20	3.5	3.0	20.26	
		F	8	2.0	1.0	20.58	
		G	15	2.5	2.5	20.66	
	Rolled bar (Lateral lug)	H	12	3.4	3.0	19.83	
		I	15	3.3	3.5	19.48	
	Rolled bar (Diagonal lug)	J	30	5.1	5.0	20.64	
		K	30	5.5	6.2	20.27	
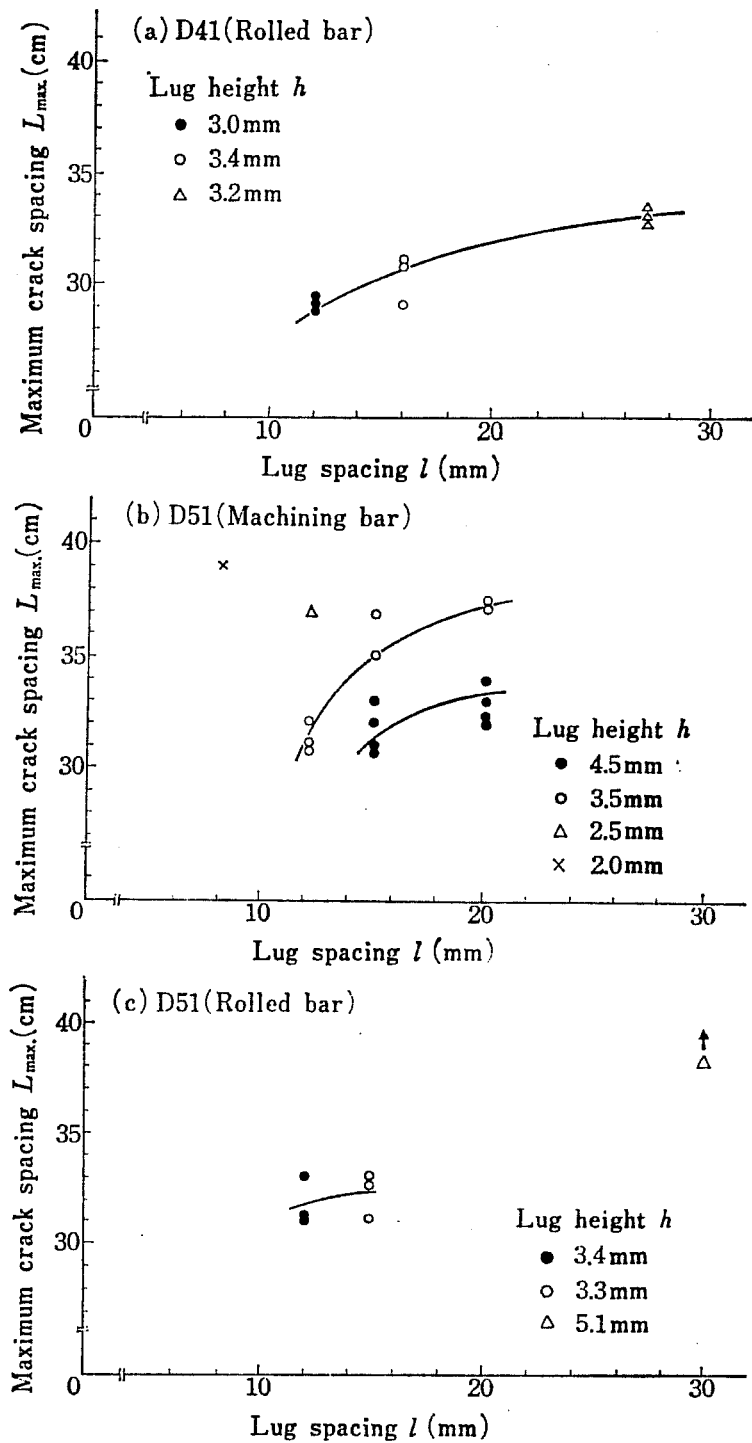
Figure 2.11 Relation between lug spacing and
maximum crack spacing
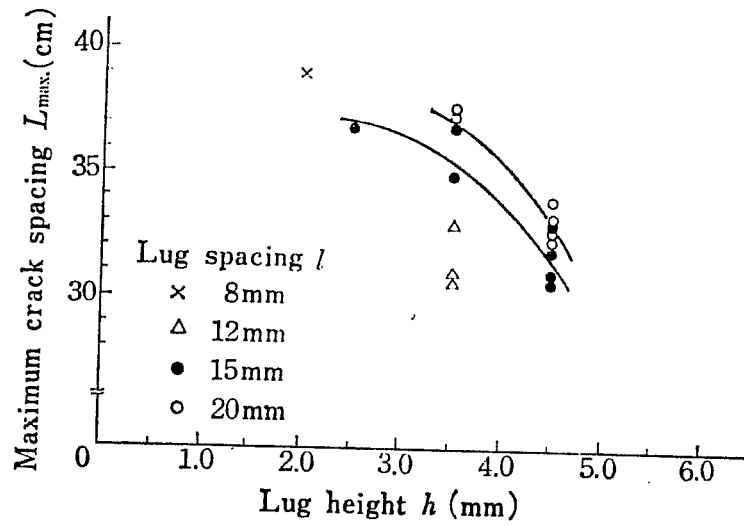
Figure 2.12 Relation between lug height and maximum crack spacing (D51 machined bars)
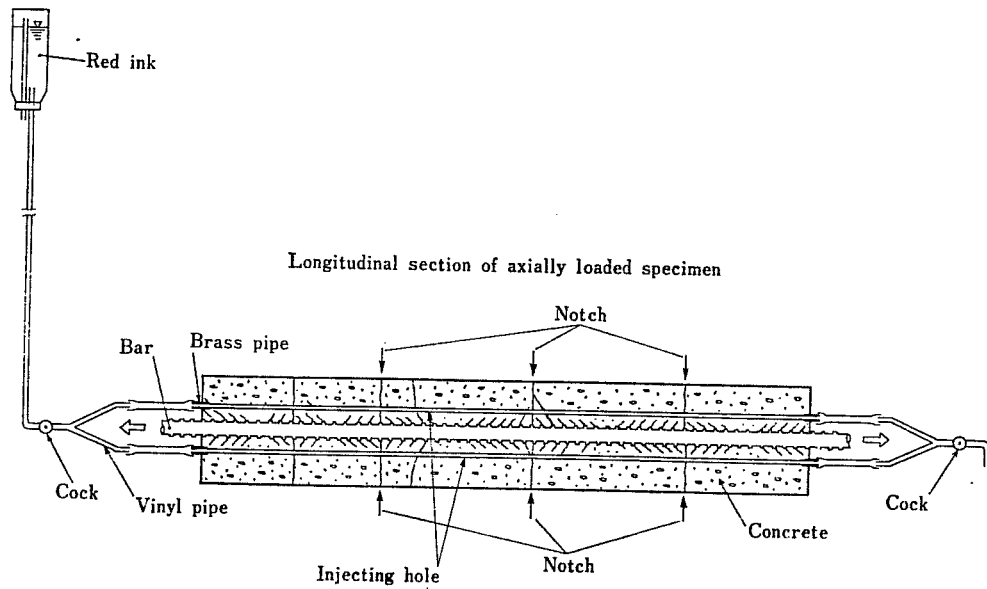
Figure 2.13 Equipment for ink injection

Type Q

Type R

Type S

(a) D41 (Rolled bar)

Type C

Type A

Type B

(b) D51 (Machining bar)

Type H

Type I

Type J

(c) D51 (Rolled bar)
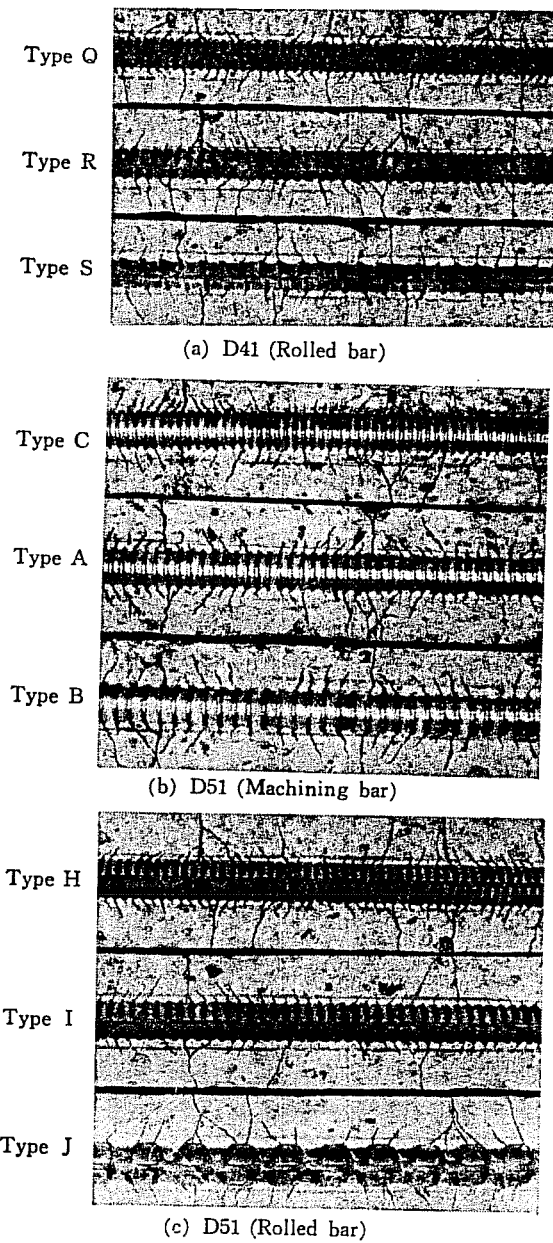
Figure 2.14 Internal cracks

20

4] Akasi,J., Fujii,S. and Morita,S.,"Effect of Concrete Strength and Bar Deformation on Bond Behavior", Proceedings of the Japan Concrete Institute, Vol.13, 1991. (in Japanese)

Akasi, Fujii and Morita conducted two types of pullout tests (Series 1 and Series 2) as shown in Fig.2.15. Specimens of Series 1 were 225 mm cubes with a steel bar positioned at the center. There was no reinforcement in the cube. Specimens of Series 2 were identical to Series 1 except that the cubes were placed in steel tubes. Concrete was cast in the gaps between the cube and confining tube. The bars had varying rib geometries. Two rib heights (h) of 2.5 and 1.3 mm ($0.1d_b$ and $0.05 d_b$), and three rib spacings (l) of 25.4, 17.8 and 10.2 mm ($1.0 d_b$, $0.7 d_b$ and $0.4d_b$) were incorporated to produce six different deformation patterns. Specimens with three different concrete strengths (L: 300 kg/cm^2 ; 29.4 MPa, M: 600 kg/cm^2 ; 58.8 MPa and H: 900 kg/cm^2 ; 88.3 MPa) were cast using each deformation pattern. The test results are summarized as follows.

1) The stiffness of τ-S curves for specimens with h/l ratio larger than 1/8 were nearly the same. However, the stiffness decreased as h/l decreased to values less than 1/8.

2) The stiffness and the bond strength at splitting as indicated by bond-slip curves increased with concrete strength (Fig.2.16).

3) The effect of the rib deformation pattern on bond characteristics can be evaluated by bearing stress-slip curves rather than bond stress-slip relation. A bearing stress-slip model was proposed.

4) Maximum shear strength under sufficient confinement to prevent splitting is proportional to the 0.85 power of concrete strength (Fig.2.17).

5) The concrete strain perpendicular to the bar axis at a given bond stress increased as h/l decreased.
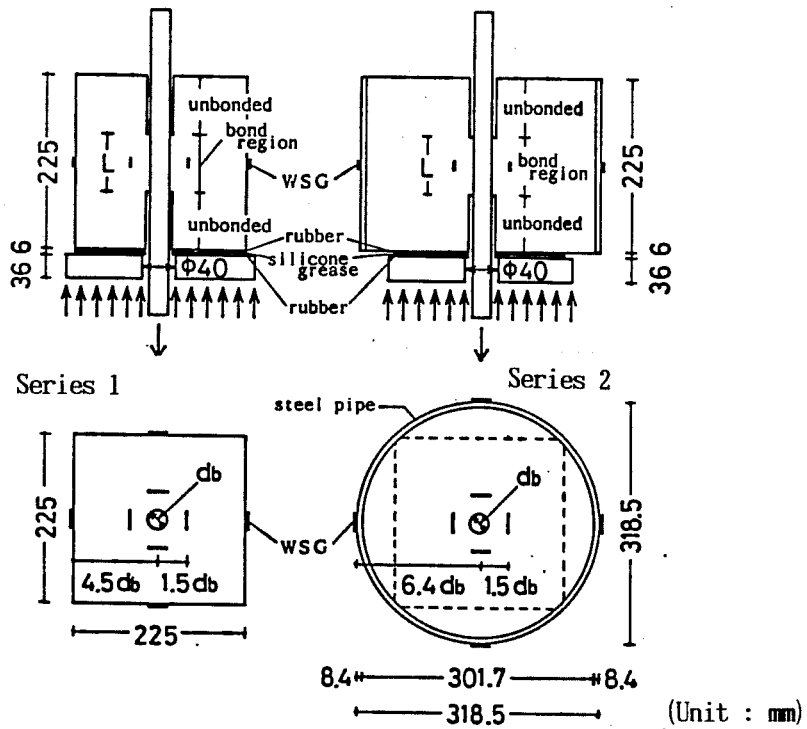
Figure 2.15 Details of specimen
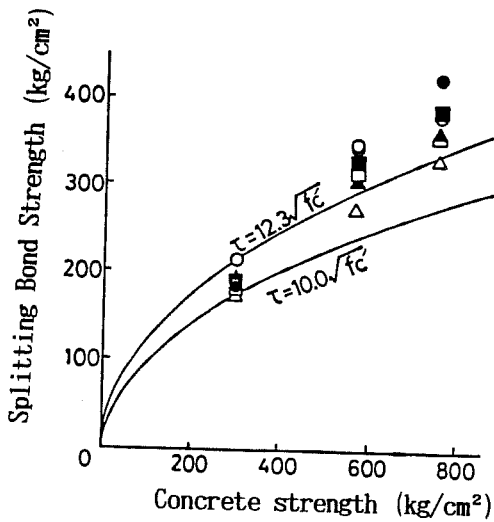
Figure 2.16 Effect of concrete strength on bond strength at splitting
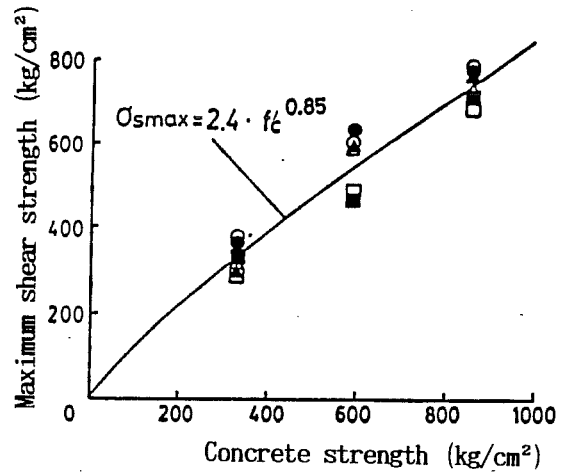
Figure 2.17 Relation between maximum shear strength and concrete strength

CHAPTER 3

Comparison between US and Japanese requirements for bar deformations

In Japan, requirements for bar deformations are described in JIS G3112 (Japan Industrial Standard). The JIS G3112 is almost the same as ASTM A615. Therefore, Japanese commercial deformed bars meet ASTM A615. The requirement in JIS G3112 are listed below. Items marked * are not found in ASTM A615.

① Deformations shall be spaced along the bar at substantially uniform distances. The deformations on opposite sides of the bar shall be similar in size and shape.

② The deformations shall be placed with respect to the axis of the bar so that the included angle is not less than 45° .

③*The roots of the ribs in deformed bars with nominal diameters exceeding 16 mm shall have a shape which does not produce concentrations of stress.

④ The average spacing or distance between deformations on each side of the bar shall not exceed seven tenths of the nominal diameter of the bar.

⑤ The summation of gaps between the ends of the rib shall not exceed 25 % of the nominal perimeter of the bar. Where the ends terminate in a longitudinal rib, the width of the longitudinal rib shall be considered the gap.

⑥ The rib height shall conform to the requirements prescribed in Table 1.

Table 1 Requirements for rib height

Bar designation No.	Rib height	
	Minimum	Maximum*
D13 or smaller	4.0% of the nominal bar diameter	twice the minimum value
larger than D13 and smaller than D19	4.5% of the nominal bar diameter	twice the minimum value
D19 or larger	5.0% of the nominal bar diameter	twice the minimum value

* not found in ASTM A615

There were some additional proposals for requirements for deformation patterns of D51 bars as follows.

ⓐ Rib height of D51 bars should be 2.8 to 5.6 mm.

ⓑ The relationship between rib spacing and rib height should satisfy the following equation.

$$\frac{h}{P} \times \frac{1 - A}{1} \geqq 0.1$$

h : rib height (mm)
P : rib spacing (mm)
1 : nominal perimeter of the bar (cm)
A : summation of the gap between the ends of the deformation

However, these proposals were postponed because there was not enough data on which to base a decision.

CHAPTER 4

Deformation patterns for large size deformed bar (D51) in Japan

Since the beginning of the 1970s, the need to use large size deformed bars has been increasing in Japan. Because of concern for the bond characteristics of large bars, many research studies were conducted. This resulted in the "Design guideline for reinforced concrete structures using large size (D51) deformed bar" issued by JSCE in 1977. Steel bar makers developed large size bars with appropriate deformation patterns based on the research work. Table 2 shows the deformation patterns of these bars compared with the JIS requirement.

Table 2 Deformation patterns of D51 commercial bars (Figure 4.1)

	Weight (kg/m)	Nomi. Dia. (mm)	Cross Sect. (mm²)	Nomi. Perim. (mm)	Rib* Space (mm)	Rib* Height (mm)	Gap** (mm)
SU-D51	15.9	50.8	2027	160	30.0 (0.59)	4.5 (0.089)	36.0 (0.225)
DA-D51	15.9	50.8	2027	160	30.3 (0.60)	4.7 (0.092)	21.2 (0.133)
RE-D51 NK-D51	15.9	50.8	2027	160	15.0 (0.30)	3.5 (0.068)	14.4 (0.090)
JIS G3112 req.	15.9	50.8	2027	160	35.6 (0.70 or less)	2.5-5.0 (0.05- 0.10)	40.0 (0.25 or less)

* Values in parentheses show ratio to nominal diameter
** Values in parentheses show ratio to nominal perimeter

Figure 4.1 shows deformation patterns and bond stress - slip curves for D51 bars. The deformation patters are different from those of smaller size bars. Pull-out tests were performed using the method proposed by JCI (same as Kokubu & Okamura's method). "RE-D51" and "NK-D51" show the best bond characteristics among the three but lower fatigue resistance (Figure 4.2).

Rib section
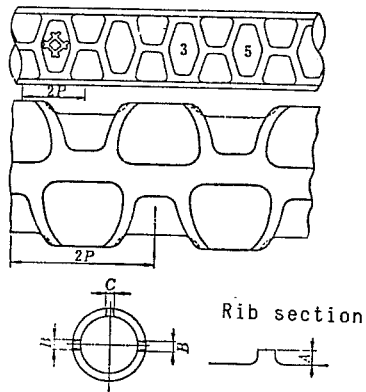
Rib spacing (P) = 30 mm
Rib height (A) = 4.5 mm
Gap (B) = 36 mm

(SU–D51)

X-X section
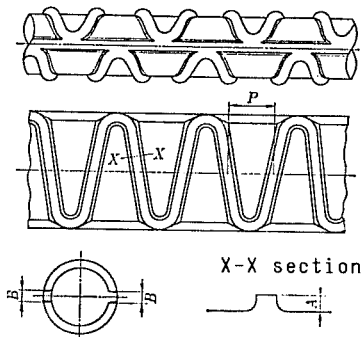
Rib spacing (P) = 30.3 mm
Rib height (A) = 4.7 mm
Gap (B) = 21.2 mm

(DA–D51)
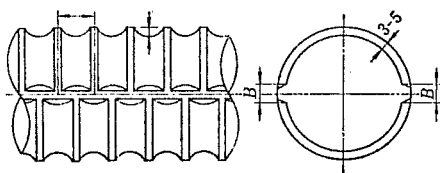
Rib spacing (P) = 15 mm
Rib height (A) = 3.5 mm
Gap (B) = 14.4 mm

(RE–D51)
(NK–D51)

fc'=36 MPa

average of five specimens

fc'=37 MPa
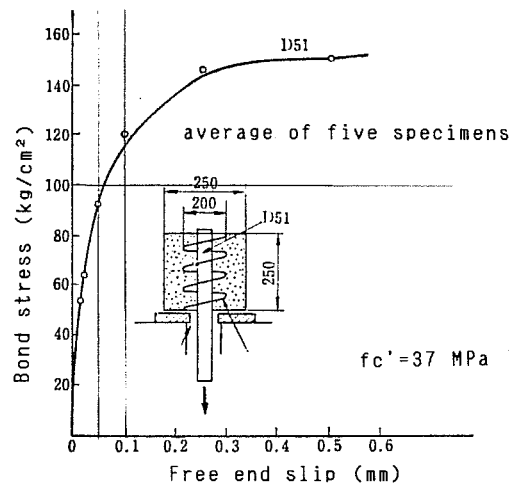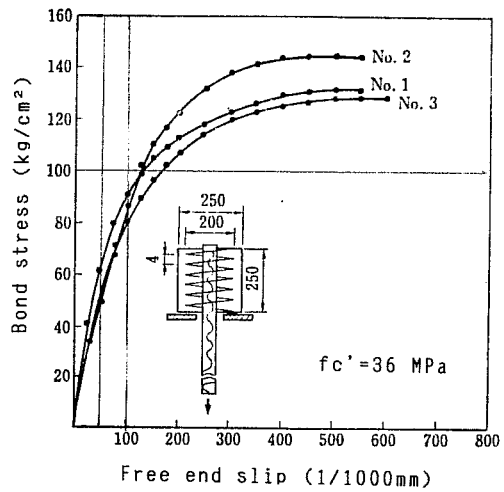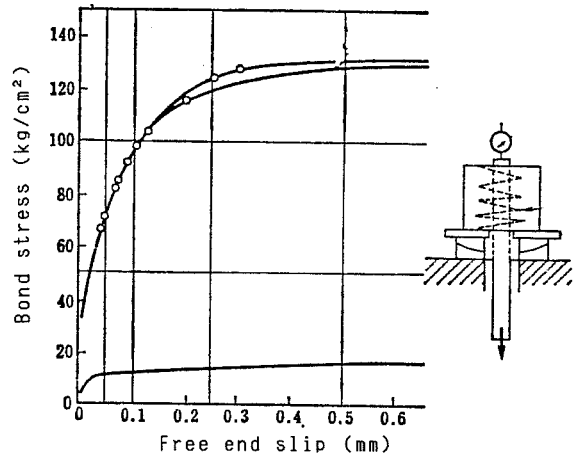
Figure 4.1 Deformations and bond-slip curves of D51 commercial bars
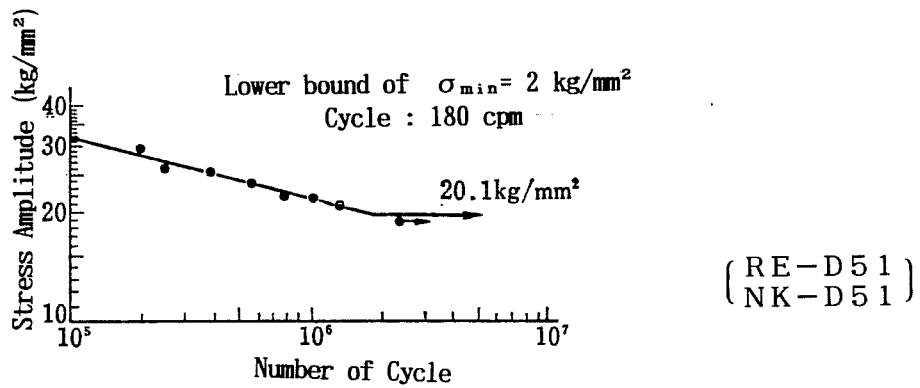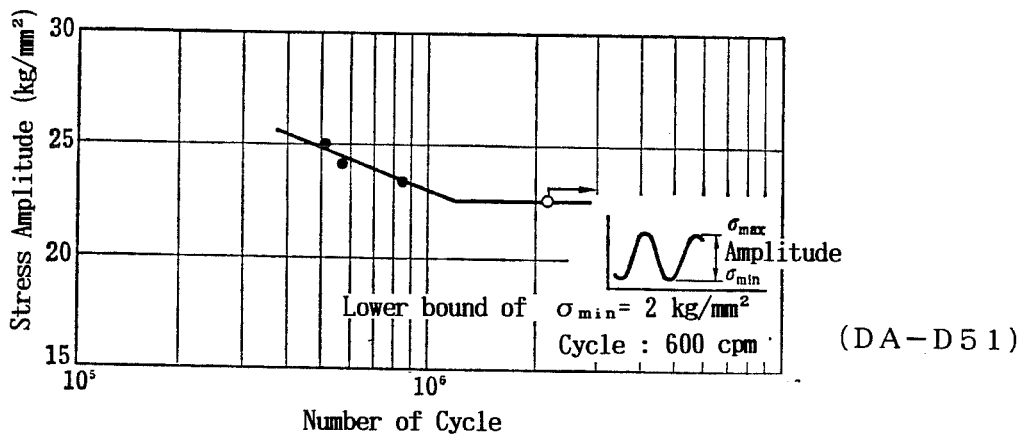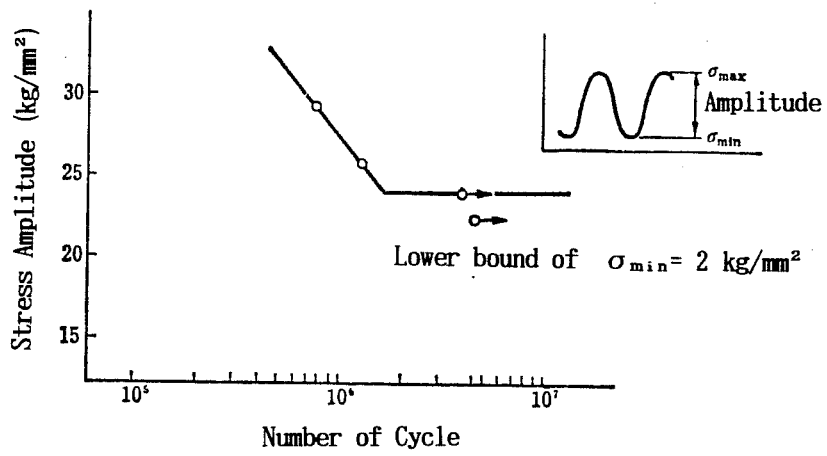
Figure 4.2 Results of fatigue tests for D51 commercial bars
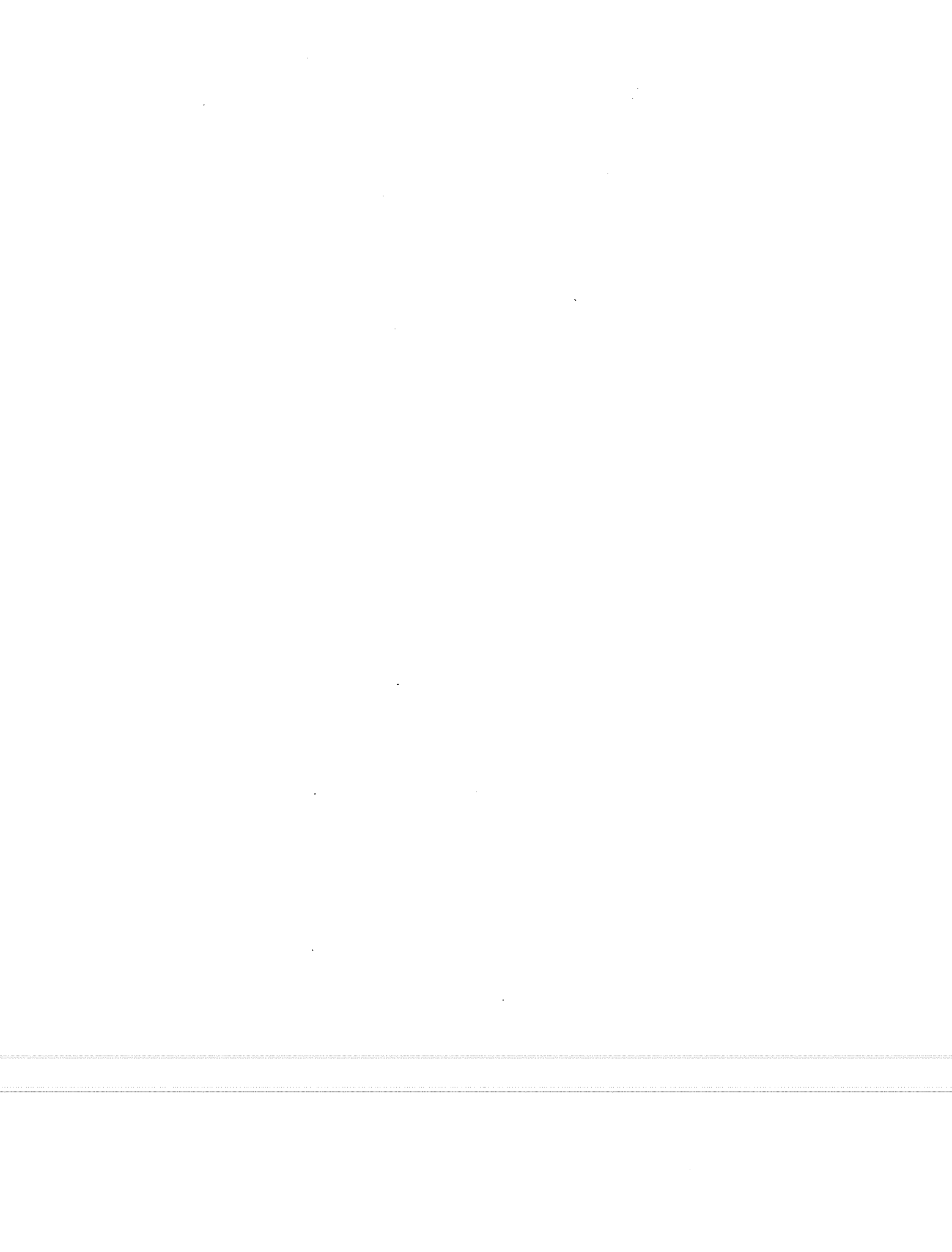
CHAPTER 5

Pullout test specimens

Pullout test using specially machined bars and commercially manufactured bars was conducted. The standard JCI (Japan Concrete Institute) test method (see Kokubu & Okamura[14]) was modified. A debonded length at the loaded end of specimens was considered.

Specimens were 200 mm cubes reinforced with spiral hoops and bars were placed at the center of cubes as shown in Fig.5.1 and Photo 5.1. Concrete was cast with the bars in a horizontal position (Photo 5.2). Most of the specimens were reinforced with spiral hoops; 6 mm plain bars with a pitch of 40 mm. The diameter of spiral hoops measured from out to out was 160 mm. Both ends of the spiral hoop were closed by welding. Some specimens had no spiral hoop to investigate the confinement by a spiral hoop. A 50 mm length at the loaded end of the bar was debonded to eliminate stress concentration.
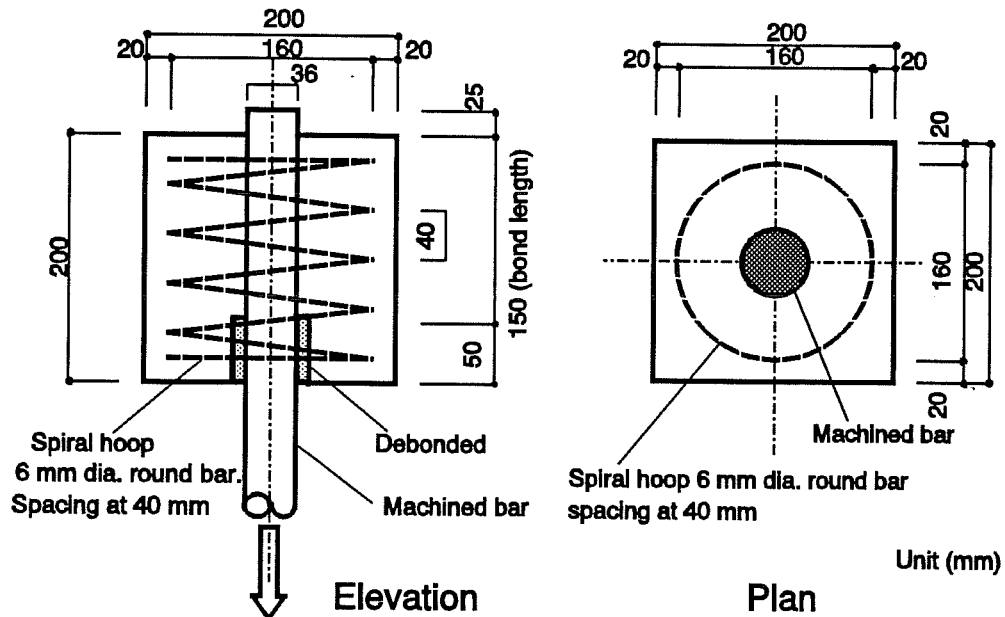
Figure 5.1 Details of test specimen

Three levels of concrete strength were used ; 40, 80 and 120 MPa (6000, 12000 and 17000 psi). Fly ash was used for 80 and 120 MPa concrete and silica fume was added to 120 MPa concrete. Coarse aggregate with a maximum size of 10 mm was used for all the concretes. The design mix proportions per cubic yard are shown in Table 5.1.

Table 5.1 Concrete mix proportion per cubic yard

	Specified Concrete Strength		
	40 MPa	80 MPa	120 MPa
Cement Type	II	I	I
Max. Aggregate Size (in.)	3/8	3/8	3/8
Water (lb.)	280	270	222
Cement (lb.)	562	676	586
Coarse Aggregate (lb.)	1625	1665	1943
Fine Aggregate (lb.)	1475	1248	1188
Fly Ash (lb.)	---	254	313
Silica Fume (lb.)	---	---	100
Superplasticizer (oz)	20	160	268
W/(C+F)	0.50	0.29	0.25
Compressive strength of 100x200-mm cylinders at 28 days (MPa)	38.5	87.6	108.8
Compressive strength of 100x200-mm cylinders at test (MPa)	38.3 (37 days)	82.9 (12 days)	115.4 (47 days)
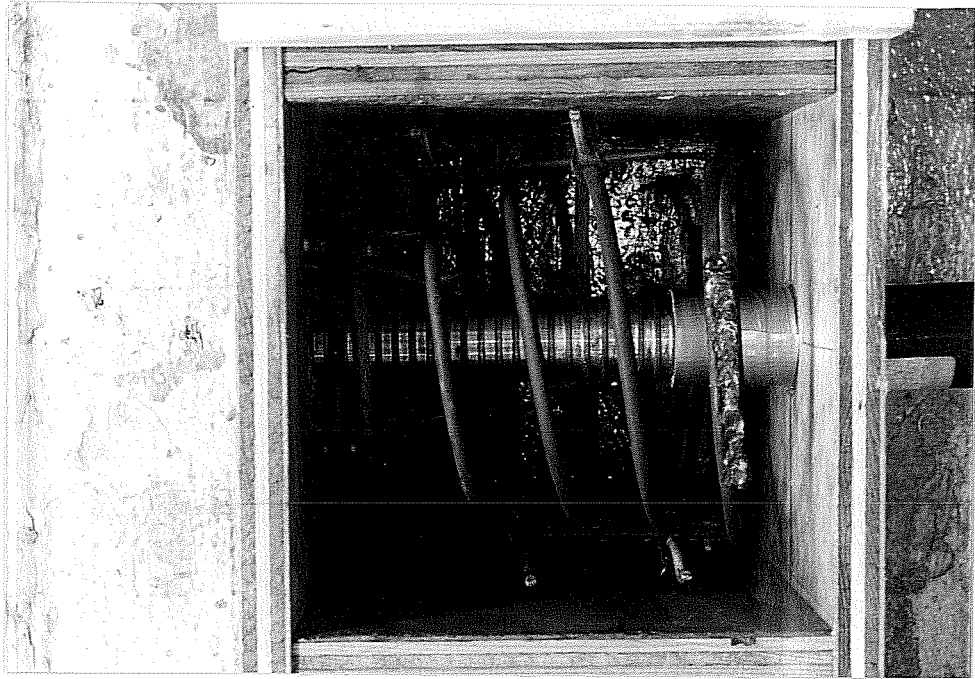
Photo 5.1 Formwork details of specimen

Photo 5.2 Concrete cast in specimens

The bars were machined from plain bars (A193 GRADE B7, f_y=620 MPa) with diameter of 44.45 mm as shown in Photos 5.3 and 5.4. The bars simulated bamboo type deformation. Table 5.2 lists details of bar deformation patterns. Notations for the deformation pattern and the specimens are also given in Table 5.2. Main variables were rib height (h) and rib spacing (ln). The nominal dimensions of machined bars were determined so that the weigh per unit length was equivalent to that of # 11 bar of ASTM specification. Therefore, the nominal diameter (D) of 35.8 mm (1.41 in.) was used for all machined bars. Rib face angle (θ) of 60 degrees and a top width of rib of 0.05D were taken as base values. Rib height (h) and rib spacing (ln) were systematically varied as shown in Fig.5.2. Rib height (h) ranged from 0.05D to 0.11D and rib spacing (ln) ranged from 0.2D to 0.8D. Fourteen combinations were selected from these ranges. Bamboo shaped #11 commercial bars (C.B.) were also used. The requirements of ASTM and JIS (Japan Industrial Standard) for bar deformation of #11 bar are noted in Fig.5.2. The maximum rib spacing shall not exceed 0.7D in both ASTM and JIS. For rib height, ASTM specifies only the minimum rib height of 0.05D. On the other hand, JIS has the requirement for both the minimum and the maximum rib height of 0.05D and 0.1D. Photos 5.5, 5.5 and 5.7 show machined bars. In each Photo, bars have the same rib height and the spacing between ribs is varied.

For specimens with concrete strengths of 80 and 120 MPa, seven specimens were added to investigate the following.

① To investigate the effect of spiral hoop, specimens of #3, 7, 11 and commercial bar without spiral hoop were made.
② To investigate the effect of rib face angle, the bars with same rib height and rib spacing as the commercial bar but different rib face angle of 30, 45 and 60 degrees were machined as shown in Photo 5.8. It should be notice that the rib face angle of commercial bar was 30 degrees. Photo 5.9 shows the cross section of a commercial bar.

Table 5.2 Detail dimensions of bars

Bar Number	ln (mm)	h (mm)	d (mm)	ln/D	h/D	h/ln	θ (degree)	Bearing Area (mm2)	Shear Area (mm2)
# 1	7.1	1.8	34.3	.2	.05	.25	60	4231	13318
# 2	10.7	1.8	34.8	.3	.05	.17	60	2860	14997
# 3	14.2	1.8	35.1	.4	.05	.13	60	2057	15096
# 4	10.7	2.8	34.0	.3	.08	.27	60	4526	15493
# 5	14.2	2.8	34.3	.4	.08	.20	60	3255	15394
# 6	18.0	2.8	34.8	.5	.08	.16	60	2640	16500
# 7	21.6	2.8	34.8	.6	.08	.13	60	1980	15082
# 8	25.1	2.8	35.1	.7	.08	.11	60	1661	14917
# 9	10.7	4.1	32.8	.3	.11	.37	60	6583	15990
# 10	14.2	4.1	33.5	.4	.11	.28	60	4800	16288
# 11	18.0	4.1	34.0	.5	.11	.22	60	3892	17226
# 12	21.6	4.1	34.3	.6	.11	.18	60	2938	15841
# 13	25.1	4.1	34.5	.7	.11	.16	60	2465	15663
# 14	28.7	4.1	34.8	.8	.11	.14	60	2481	18154
Com.Bar	24.0	1.8	34.3	.7	.052	.08	30	1209	14134
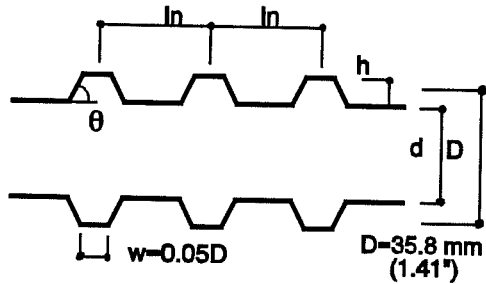
Deformation Pattern

Specimen Notation

#3 - U H

Concrete Strength
Nothing : 40 MPa
H : 80 MPa
U H : 120 MPa
Bar Number
1 - 14 & Com.Bar
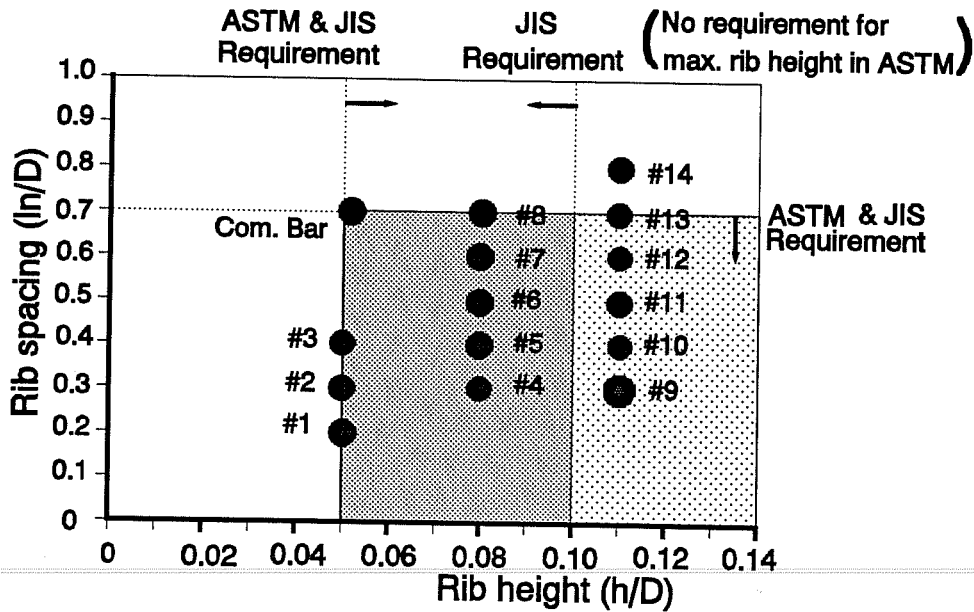
Figure 5.2 Combination of rib height and rib spacing

33
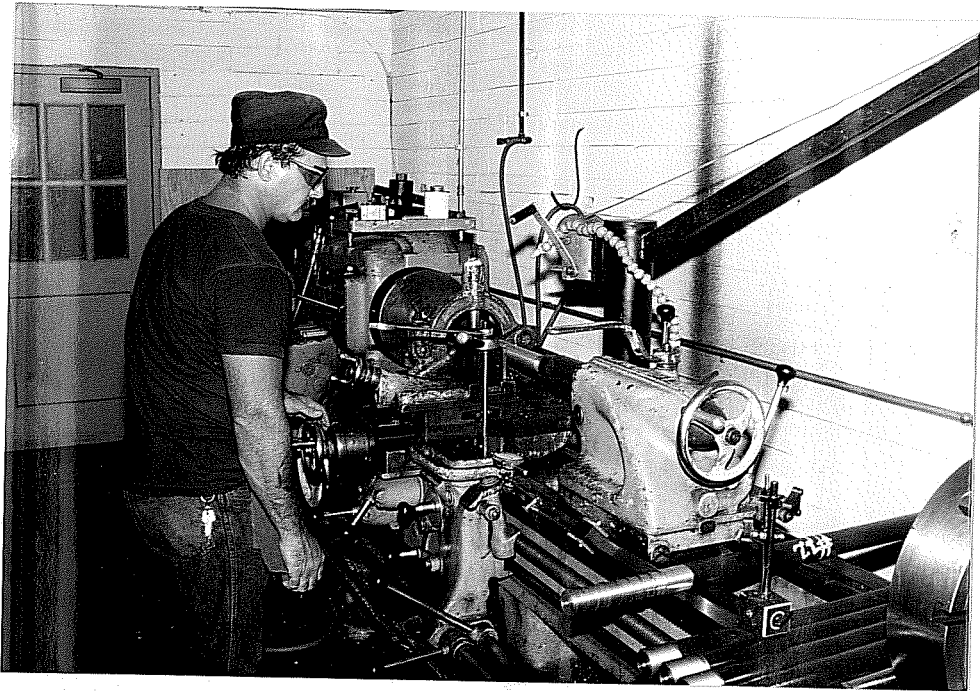
Photo 5.3 Machining of a bar
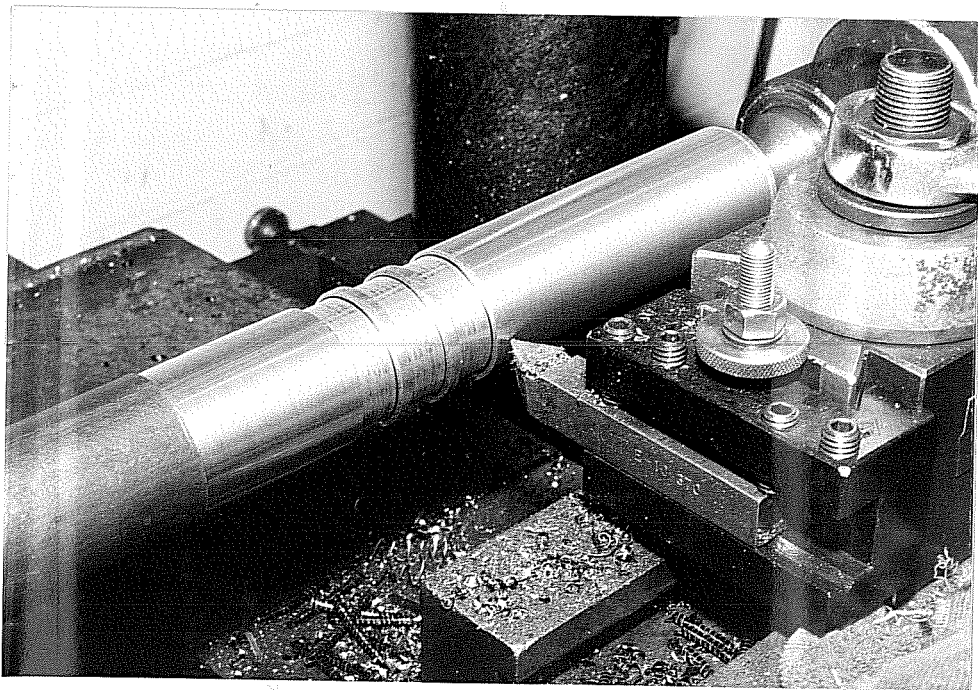
Photo 5.4 Close-up of bar machining

$\frac{h}{db}=0.05, \frac{\ell n}{db}=0.2$

$\frac{h}{db}=0.05, \frac{\ell n}{db}=0.3$

$\frac{h}{db}=0.05, \frac{\ell n}{db}=0.4$
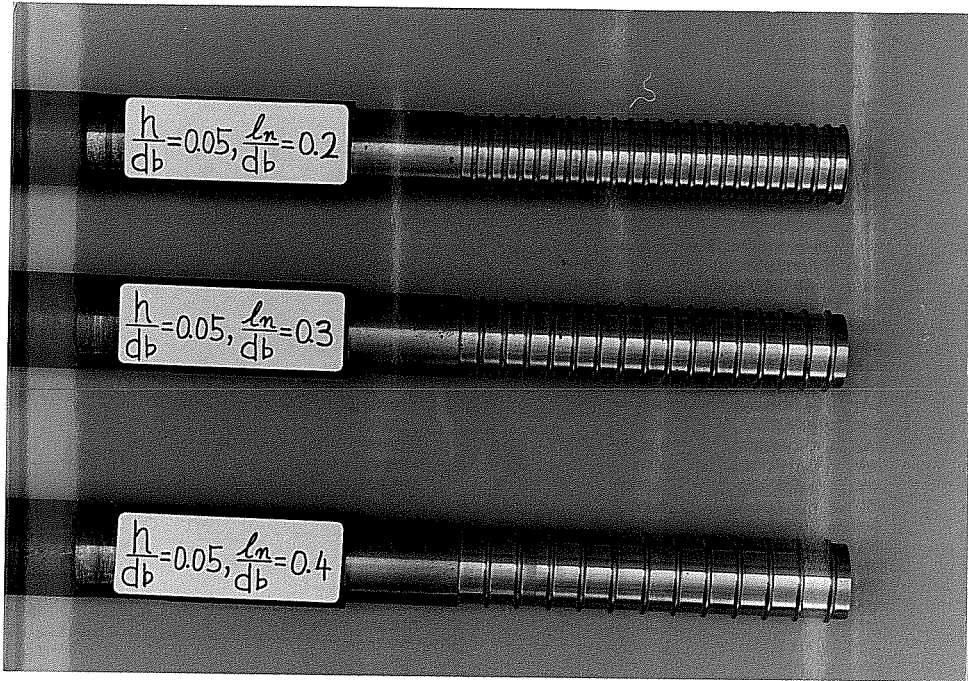
Photo 5.5 Machined bars with rib height of 0.05D

$\dfrac{h}{d_b}=0.08, \dfrac{\ell_n}{d_b}=0.3$

$\dfrac{h}{d_b}=0.08, \dfrac{\ell_n}{d_b}=0.4$

$\dfrac{h}{d_b}=0.08, \dfrac{\ell_n}{d_b}=0.5$

$\dfrac{h}{d_b}=0.08, \dfrac{\ell_n}{d_b}=0.6$

$\dfrac{h}{d_b}=0.08, \dfrac{\ell_n}{d_b}=0.7$

Photo 5.6 Machined bars with rib height of 0.08D
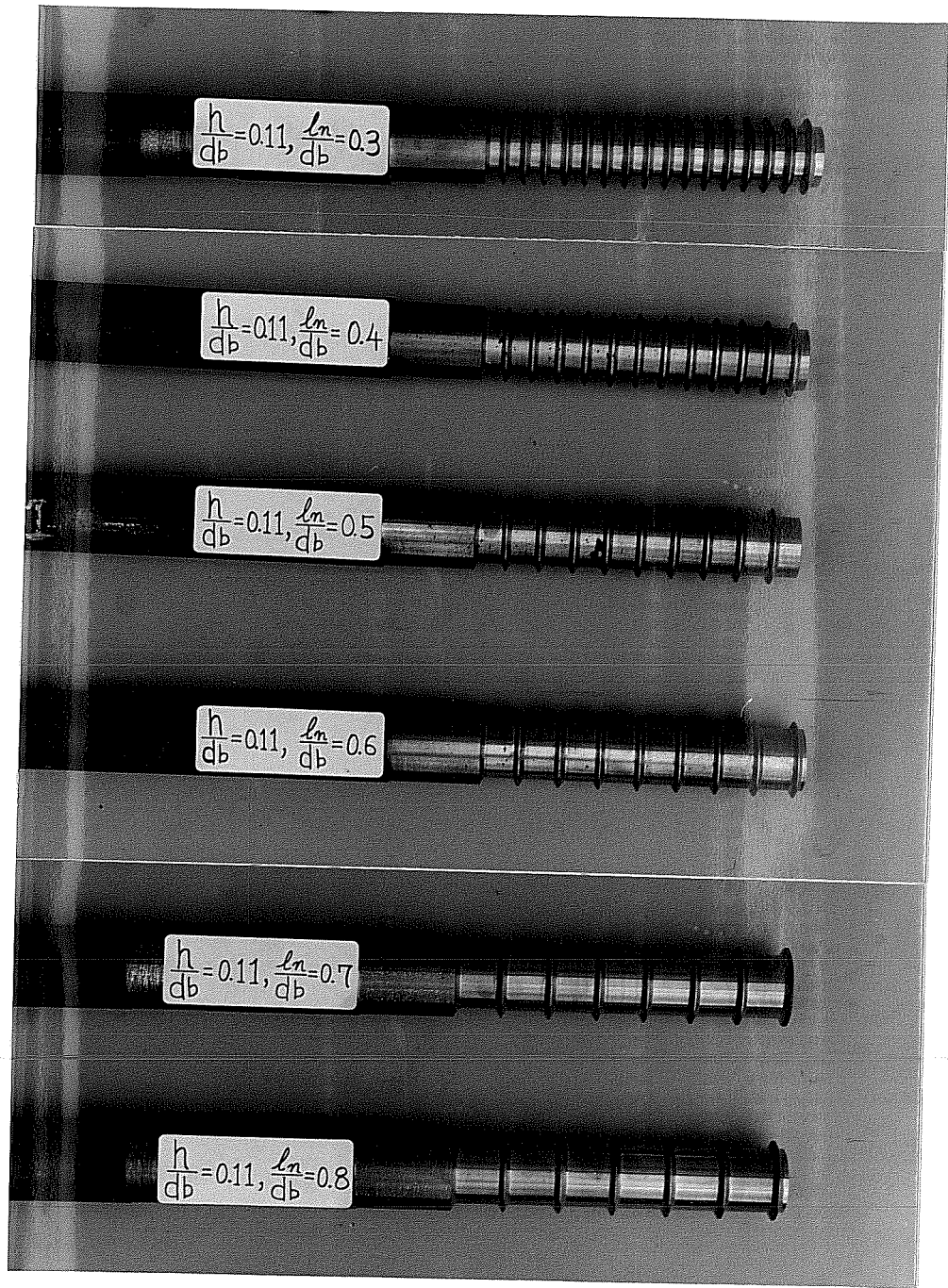
Photo 5.7 Machined bars with rib height of 0.11D
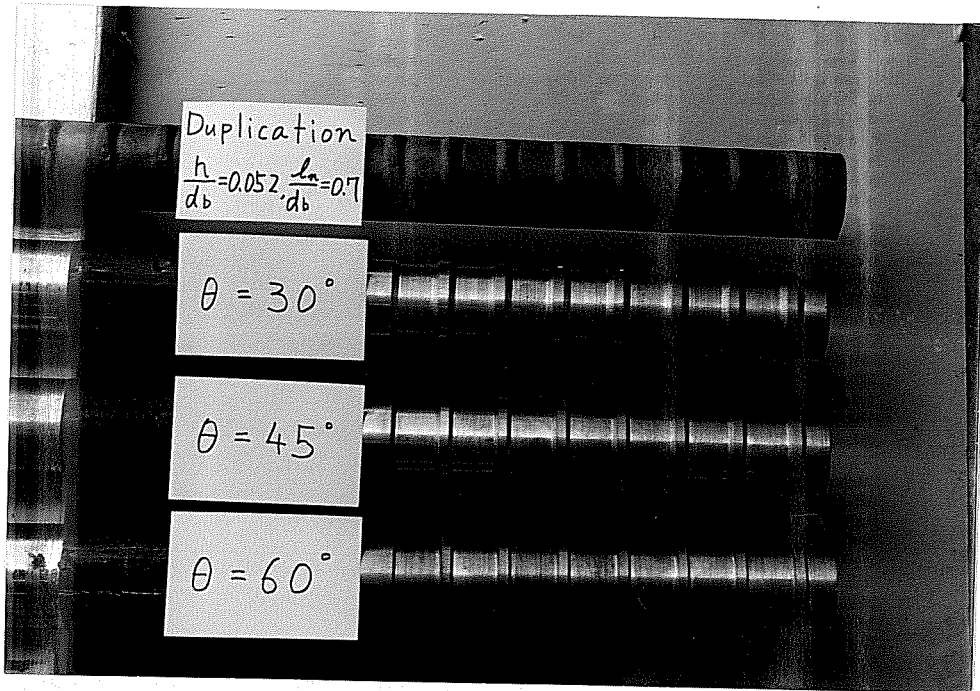
Photo 5.8 Commercial bar and duplicated bars with
rib face angles of 30 , 45 and 60 degrees
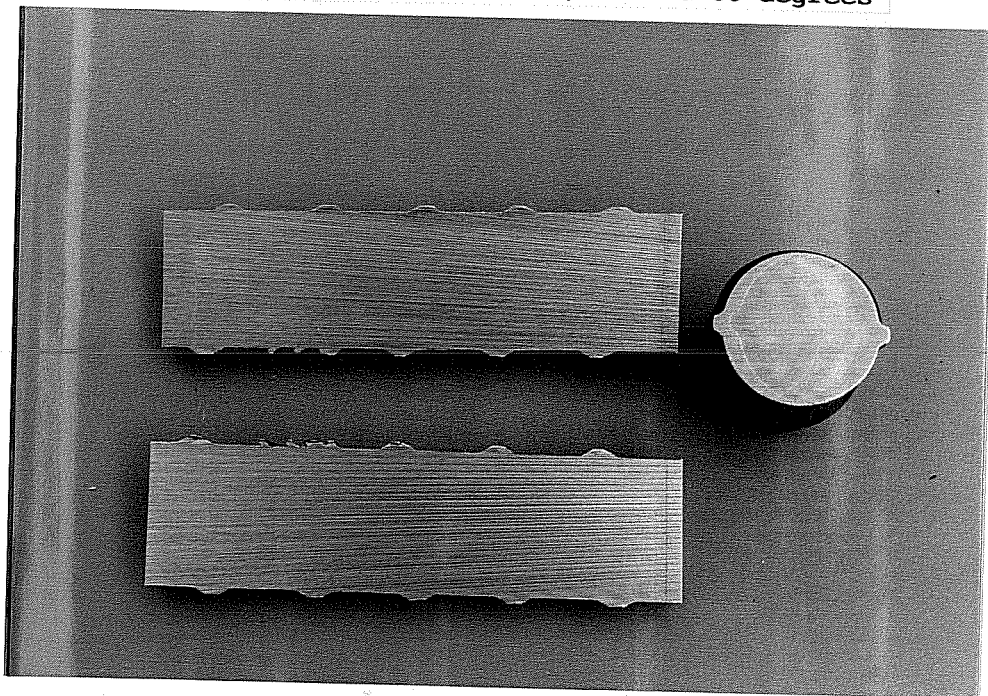
Photo 5.9 Cross section of commercial bar

CHAPTER 6

Test method

The bars were loaded with a center hole hydraulic ram with capacity of 100 t. A 25× 210× 210 mm steel plates was placed between ram and specimen as a reaction plate. The diameter of the hole in the reaction plate was 65 mm. Two Teflon sheets and a rubber sheet were positioned between the reaction plate and specimen to eliminate friction.

The load was monitored by a calibrated electronic 10,000 psi pressure transducer connected to the pressure line. The free end slip was measured by digital displacement transducer mounted on a steel frame which was attached to the specimen through inserts embedded in the concrete. Photos 6.1 and 6.2 show the test setup.
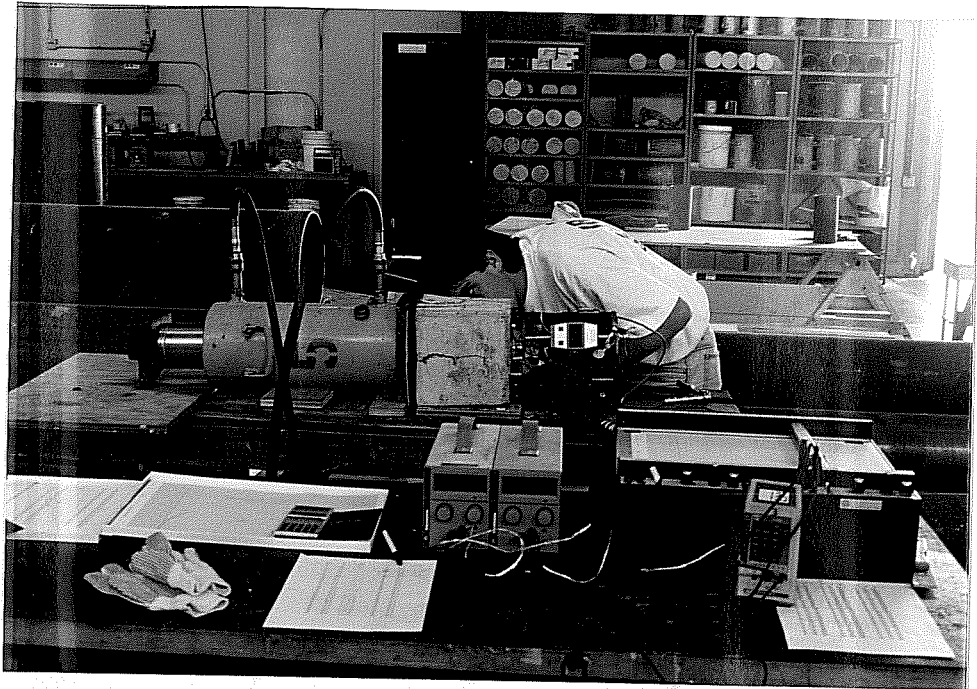
Photo 6.1 Overall view of the test setup
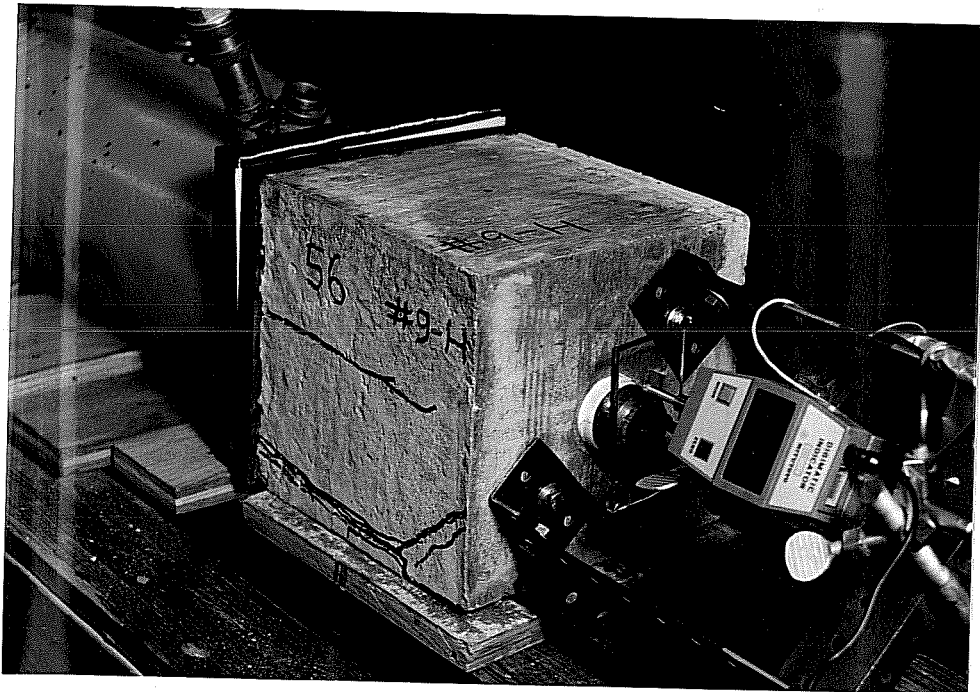
Photo 6.2 Measurement of free end slip

CHAPTER 7

Test results

7.1 General behavior

The free end slip increased gradually at early stages of loading for all the specimens. At higher levels of loading, plateaus in load-slip relations were observed except for 40 MPa concrete specimens with small rib spacing. At the loads at level of the plateaus, cracks in the cover concrete were observed for some specimens. However, for most specimens, it was difficult to find the cracks. The number of cracks increased as the load increased. Finally cover concrete outside of the spiral hoop spalled, the free end slip increased and the load dropped suddenly. For 40 and 80 MPa concrete specimens, the test was terminated at this stage. However, for 120 MPa concrete specimens, bars were loaded to larger deformations. The load increased again for larger slip and reached the maximum strength. Finally, the bars were pulled out from the cubes. It was observed for all the specimens with 120 MPa concrete that the concrete keys between ribs were sheared off (see APPENDIX).

It is felt that free end slip larger than 0.25 mm is not useful from the viewpoint of structural application. The behavior up to free end slip of 0.12 mm is discussed in this paper. The failure mode of the specimens is between splitting of the concrete and pullout of the bar in all cases. After the test, the specimens were cut and opened to investigate internal cracks. Cracks with angles of 45 to 60 degrees to bar axis and starting from the top rib were observed for most specimens. These internal cracks extended (radiated out) to the spiral hoop. Photos 7.1 and 7.2 show final appearance of a specimen and internal cracks of a specimen.
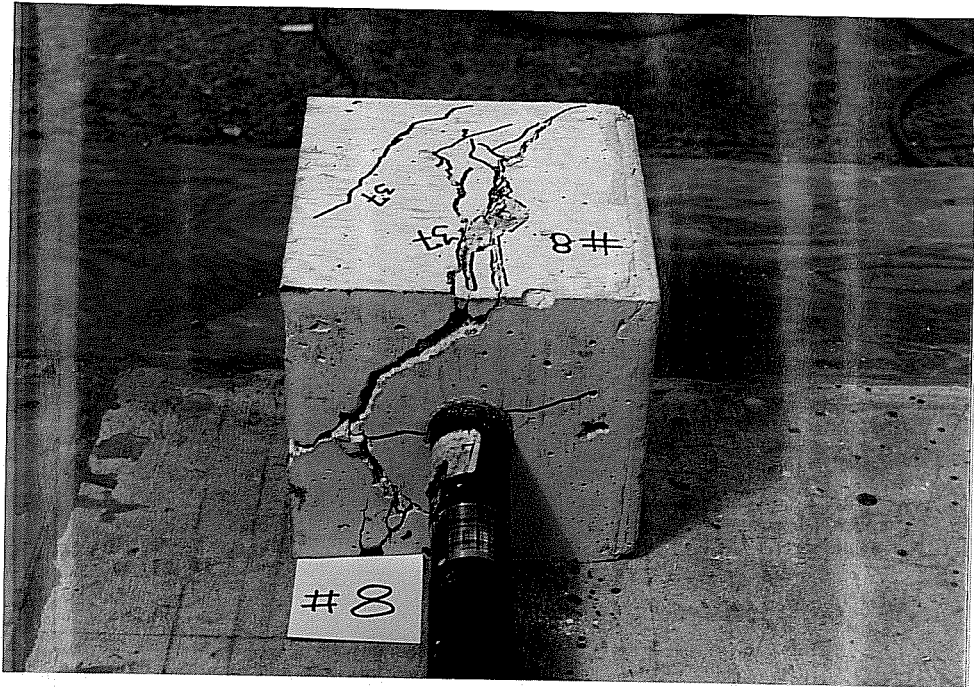
Photo 7.1 Final appearance of a specimen with 40 MPa concrete

Photo 7.2 Internal cracks of a specimen with 40 MPa concrete

7.2 Bond stress - free end slip curves

The bond stress - free end slip relations of specimens with concrete strength of 40, 80 and 120 MPa are shown in Figures 7.1, 7.2 and 7.3, respectively. Each figure includes three diagrams in which the specimens with the same rib height but different rib spacing are compared. Although there was some scatter of the data, the following general characteristics of the bond - slip curves were observed. ① The stiffness increased with the concrete strength. ② The stiffness increased as the rib spacing decreased and the rib height increased for specimens with concrete strength of 40 and 80 MPa. Comparison of 120 MPa concrete specimens with the same rib height but different rib spacing showed less difference in bond-slip curves than those with lower strength concrete. For 120 MPa concrete, the effect of rib spacing on the stiffness was unclear but the effect of rib height was significant. ③ For all the specimens with concrete strength of 80 and 120 MPa, the plateaus in bond-slip relationship which are considered to correspond to the strength at splitting, were observed. On the other hand, for specimens with concrete strength of 40 MPa and with smaller rib spacing, the plateaus were not observed.
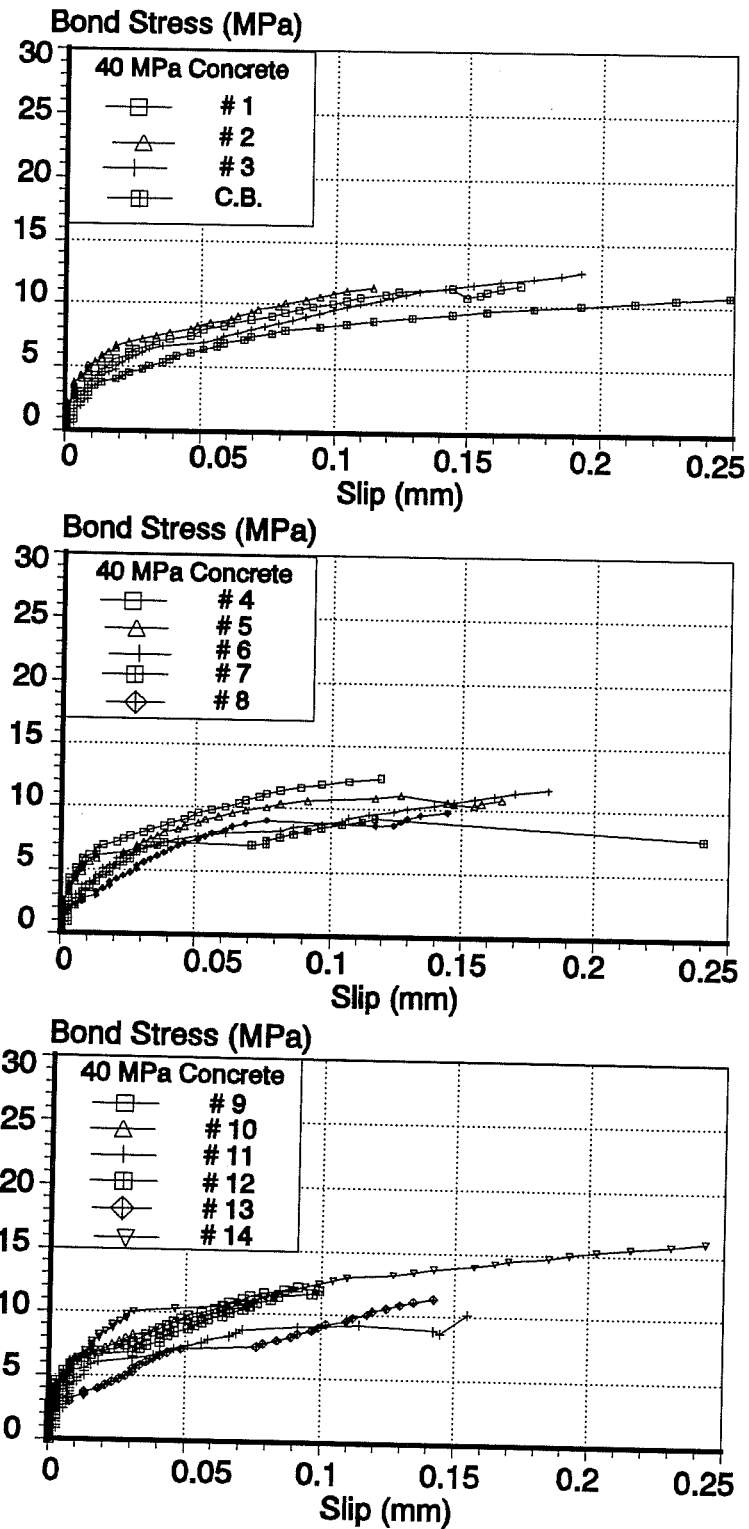
Figure 7.1 Bond stress – free end slip curves
of 40 MPa concrete specimens
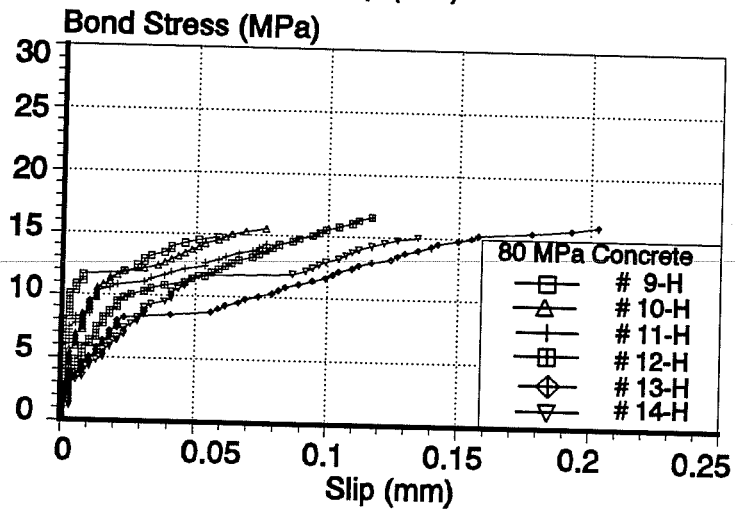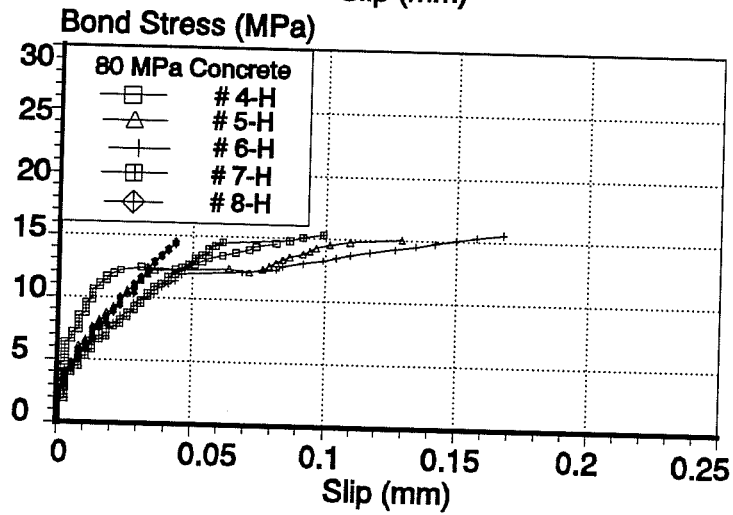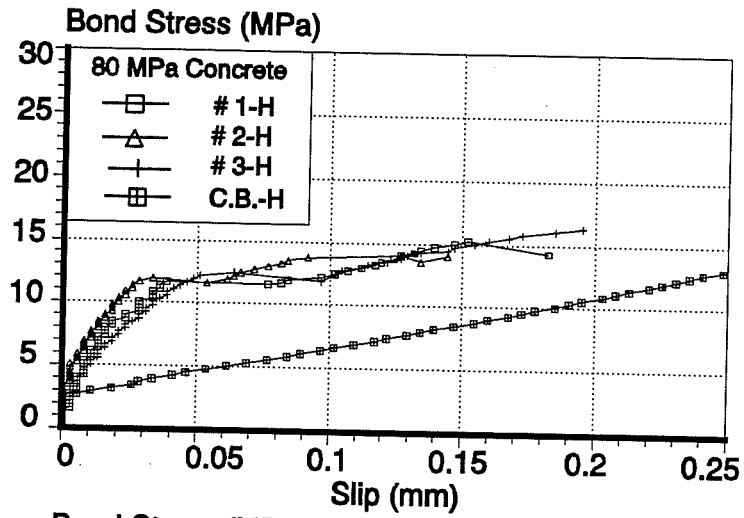
Figure 7.2 Bond stress - free end slip curves
of 80 MPa concrete specimens
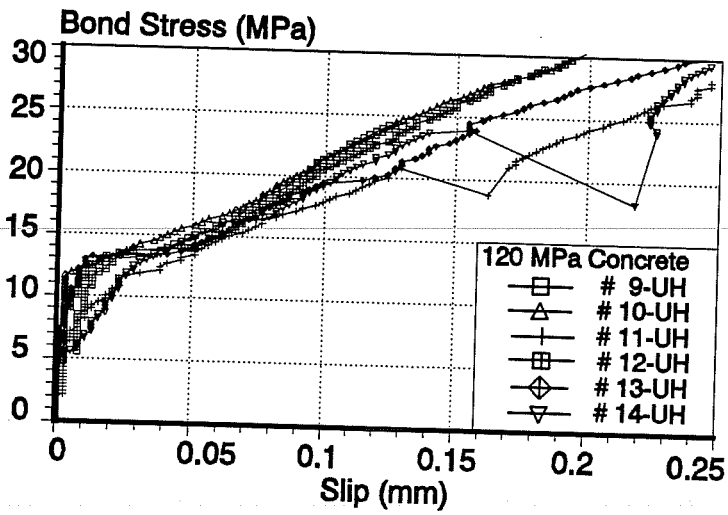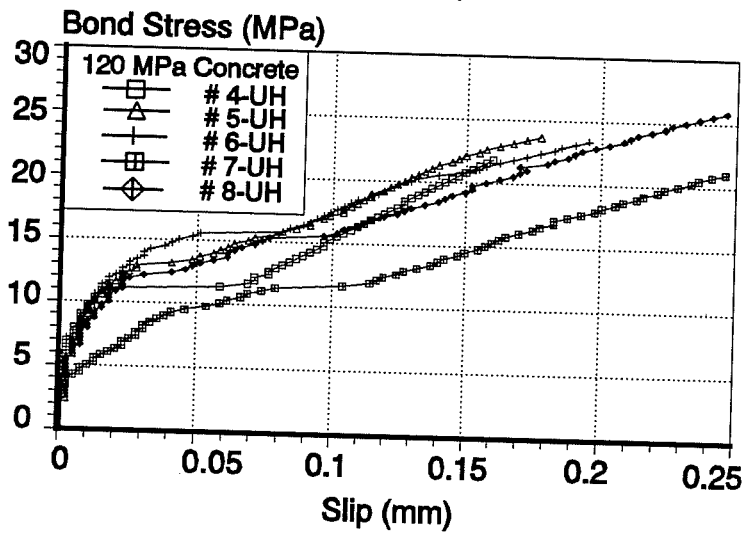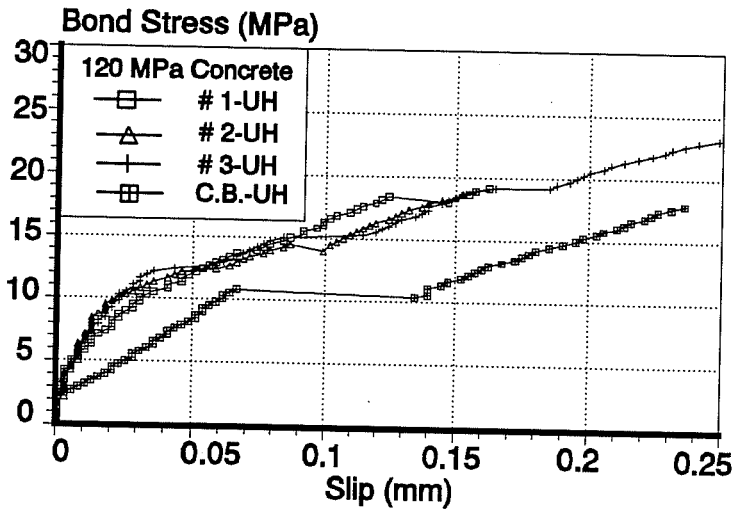
Figure 7.3 Bond stress - free end slip curves
of 120 MPa concrete specimens

Figure 7.4 shows the comparison between bond-slip curves of a commercial bar and machined bars which have the same rib height and the same rib spacing as the commercial bar but different rib face angles of 30, 45 and 60 degrees. The concrete strength is 80 MPa. The rib face angle of the commercial bar was 30 degrees. The bond-slip curves of machined bars with rib face angles of 45 and 60 degrees (Dup.45 and 60) were almost identical. However, the stiffness of the machined bar with rib face angle of 30 degrees (Dup.30) was smaller than that of 45 and 60 degrees (Dup.45 and 60). This supports the result from previous research that the rib face angle larger than 45 degrees shows little difference in bond behavior [2, 10, 12, 13 and 14]. A comparison of the commercial bar and the machined bar with identical deformation geometry shows that the bond-slip curves were almost identical.
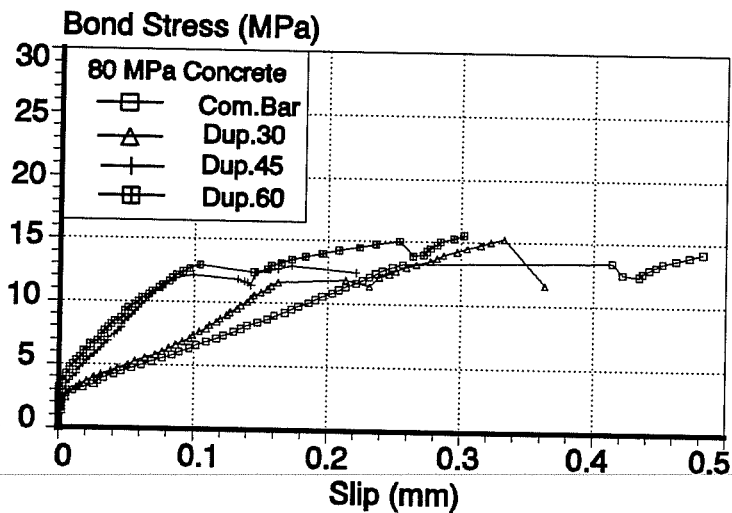
Figure 7.4 Comparison of a commercial bar and machined bars
with rib face angles of 30, 45 and 60 degrees

47

For 80 and 120 MPa concrete, specimens without spiral hoop were made for bar number 3, 7, 12 and C.B. Comparisons of the bond-slip curves with and without spiral hoop are shown in Figures 7.5 and 7.6. The specimens in the same diagram have the same bar deformation and the same concrete strength. The curve of the specimen of bar deformation #12 without spiral hoop corresponds halfway to that of the companion specimen with spiral hoop as expected for both 80 and 120 MPa concrete. However, the other specimens without spiral hoop exhibited larger stiffness than companion specimens with spiral hoop. In these specimens, the presence of spiral hoop may disturb concrete shrinkage and lead to micro cracks. The loads at first plateaus in bond-slip curves of specimens with spiral hoop approximately correspond to the maximum strength of companion specimens without spiral regardless of concrete strength. This means that the bond stress at first plateau should correspond to the first splitting of concrete.
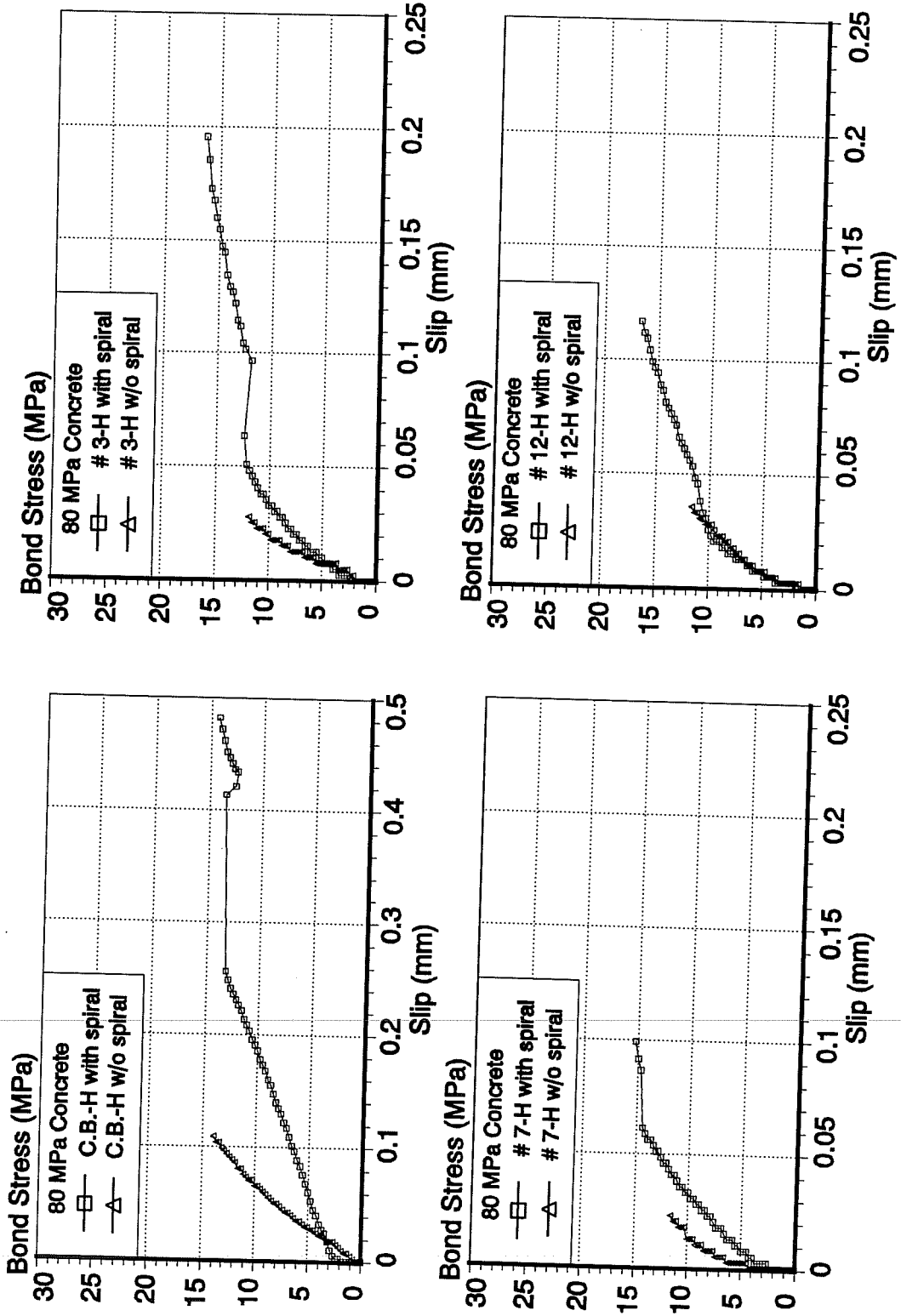
Figure 7.5 Comparison of bars with and without spiral hoop (80 MPa Concrete)

49
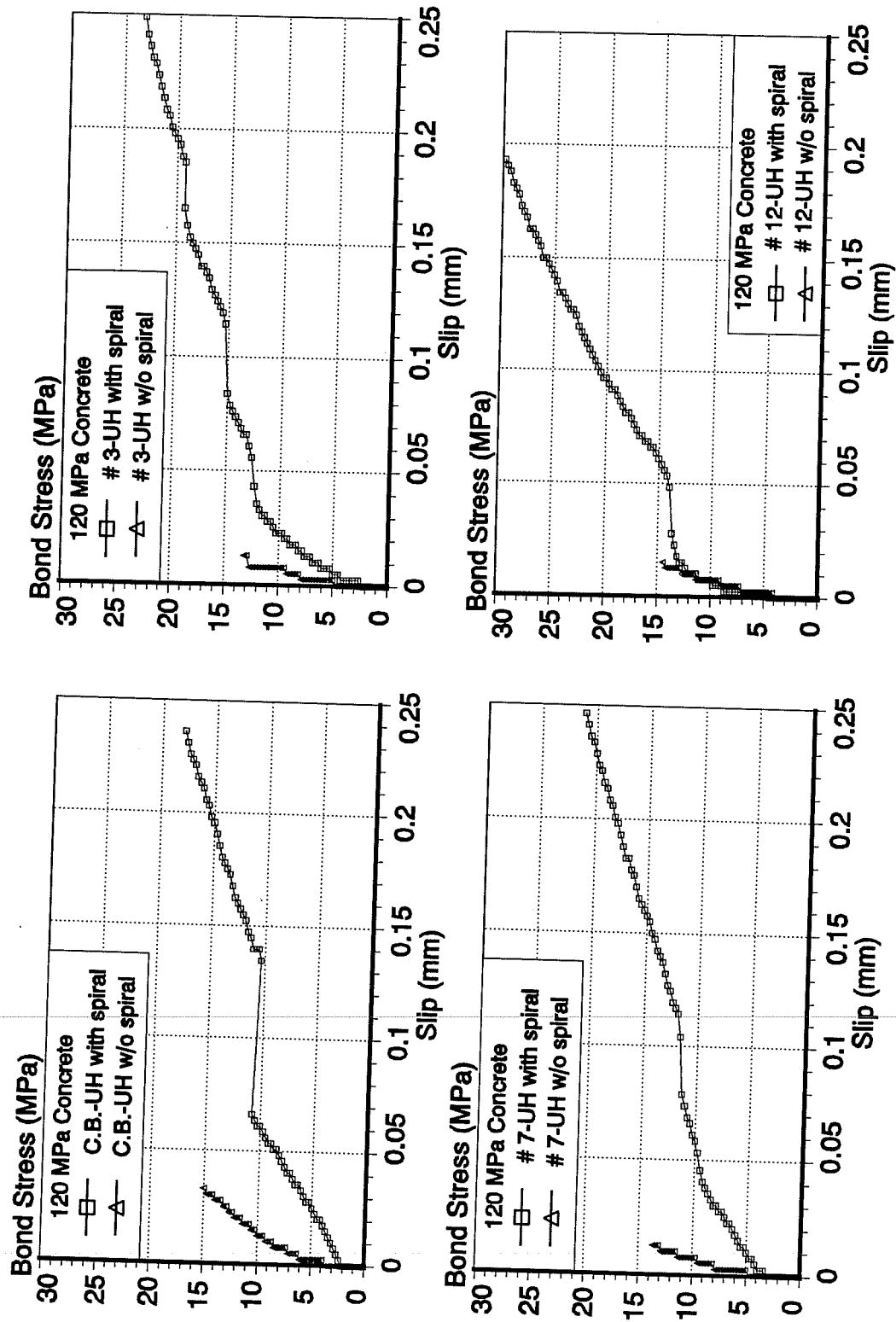
Figure 7.6 Comparison of bars with and without spiral hoop (120 MPa Concrete)

CHAPTER 8

Analysis of test results

The influence of bar deformation on bond stress, bearing stress and shear stress is examined in this section.

8.1 Relation between bond stress and bar deformation geometry

To determine good bar deformation geometry for bond, the performance criteria must be established. Improved bond behavior was defined in terms of an improvement of the stiffness and the average bond stress in the bond-slip relationship and an increase in the strength at bond splitting. The average bond stress of a bar at a range of slip values was used to obtain a comparison. The bond stresses for slip values of 0.025, 0.051, 0.076 and 0.102 mm (0.001, 0.002, 0.003 and 0.004 in.) at the free end were totaled for each specimen and divided by the number of slip values to give an average value. The initial stiffness of the bond-slip curve was defined using the bond stress at 0.0127 mm (0.0005 in.) slip or at first splitting whichever is less as shown in Figure 8.1. The bond stress for the first plateau or a large stiffness decrease in bond stress-slip curve was defined as the bond stress for the first splitting. First splitting will probably show the largest scatter because it is a somewhat subjective value.
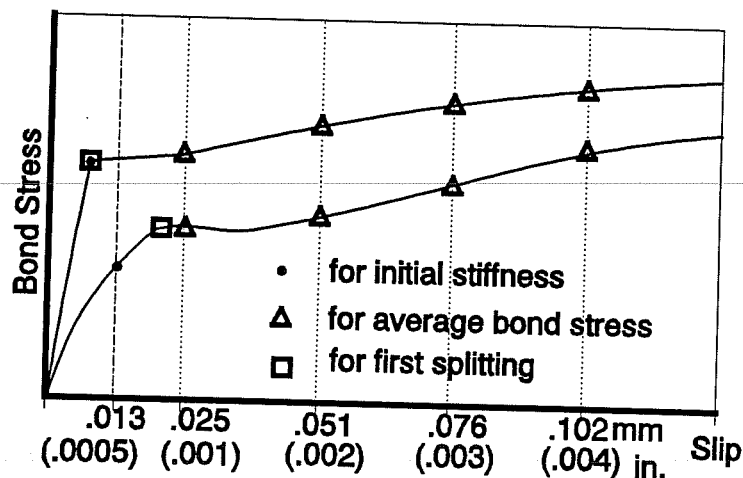
Figure 8.1 Definitions of average bond stress, initial stiffness and bond stress at first splitting

51

The bond length of all the specimens in this test was equal to 150 mm. The dimension of the bar ribs were determined so that the nominal bar diameter was equal to that of a #11 bar using ASTM specifications. Therefore, all the specimens have the same bond area of 16880 mm² (26.16 sq. in.). The bond stress (τ) is expressed as follows.

$$\tau = P \diagup (\pi D 1) \qquad \cdots\cdots\cdots\cdots\cdots (1)$$

where P is the load on the bar, D is the nominal diameter of the bar (35.8 mm or 1.41 in.) and 1 is the bond length (150 mm or 5.9 in.).

The average bond stress, initial stiffness and the bond stress at first splitting are compared in Figures 8.2 and 8.3. Bars with the same rib height or the same rib spacing are grouped together. Table 8.1 lists the test results.

Table 8.1 Test results

| Bar Number	Average Bond Stress (MPa) Concrete Strength			Initial Stiffness (MPa) Concrete Strength			Bond Stress at First Split (MPa) Concrete Strength		
	40 MPa	80 MPa	120 MPa	40 MPa	80 MPa	120 MPa	40 MPa	80 MPa	120 MPa
#1	8.34	11.50	12.98	4.48	8.17	6.33	11.07	11.60	18.45
#2	8.97	12.34	12.68	5.53	7.91	7.38	11.33	11.86	14.50
#3	7.64	11.28	13.19	3.69	5.53	7.12	6.59	12.12	12.39
#4	10.05	13.09	12.64	6.33	9.75	10.02	12.39	12.39	11.33
#5	8.95	12.32	14.71	5.80	6.85	10.02	6.06	12.12	13.18
#6	7.71	11.77	15.47	4.22	6.33	9.75	7.91	11.86	15.55
#7	7.19	12.00	9.89	3.95	5.80	5.27	7.12	14.50	11.33
#8	7.47	10.15	12.72	2.90	6.33	8.96	8.96	14.50	12.39
#9	9.44	13.24	16.90	6.33	11.60	10.81	6.85	11.60	12.91
#10	8.57	13.82	17.33	6.33	9.75	12.39	8.17	11.86	12.12
#11	7.86	12.48	14.83	5.01	9.75	8.96	6.06	10.81	12.12
#12	8.76	12.72	16.47	6.33	6.59	12.39	6.59	10.81	13.97
#13	7.12	9.71	15.85	3.43	5.27	13.18	7.12	8.17	13.44
#14	10.79	11.02	15.65	6.59	4.74	7.12	10.02	11.60	16.34
Com.Bar	6.74	5.05	8.75	3.69	2.98	3.43	10.81	12.91	10.81

1) Effect of rib spacing :

    Bars are grouped in Figure 8.2. according to rib height.
Within each group, the spacing between ribs is varied. Note that
as the specimen numbers increase, the rib spacing increases. The
specimens with a rib height of 0.05D (D: bar diameter) showed
little difference in the average bond stress and the initial
stiffness (Fig.8.2(a) and 8.2(b)). For specimens with rib height
of 0.08D and 0.11D, the average bond stress and the initial
stiffness tend to decrease (except for a few specimens) when the
rib spacing increases for concrete strength of 40 and 80 MPa.
However, the trend was unclear for concrete strength of 120 MPa.
The commercial bar (C.B.), with a deformation pattern
characterized by the lowest rib height and the largest rib
spacing allowed by ASTM, exhibited the lowest average bond stress
and initial stiffness but reasonably good bond stress at first
splitting regardless of concrete strength. The bond stress at
first splitting showed a fairly wide scatter and the effect of
rib spacing on the bond stress for first splitting is unclear
(Fig.8.2(c)).
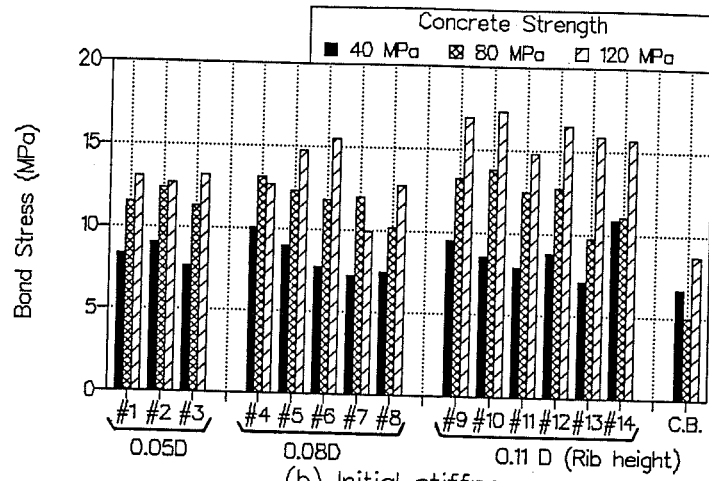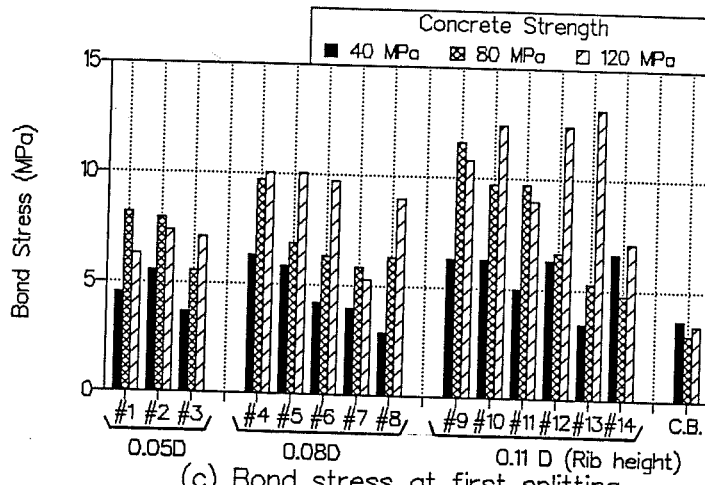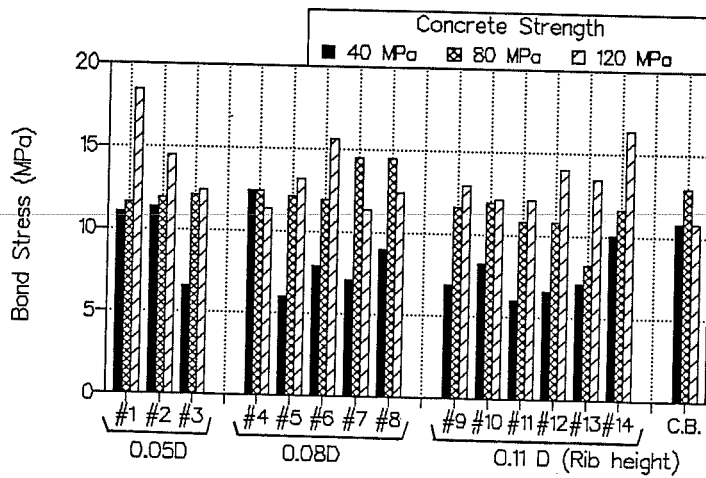
Figure 8.2 Effect of rib spacing

2) Effect of rib height :

Figure 8.3 groups specimens with the same rib spacing but different rib height. In each group, the specimens at the right-end have largest rib height. It is clear that the average bond stress and the initial stiffness increased as the rib height increased (Fig.8.3(a) and 8.3(b)). This trend is stronger for higher strength concrete. The bond stress at first splitting was not dependent on rib height (Fig.8.3(c)).

Figure 8.3 Effect of rib height

56

3) Effect of ratio of rib height to rib spacing (h/ln) :

The relationship between bond stresses and (h/ln) was analyzed. The reason for considering (h/ln) is that the effect of bearing area on bond behavior has been shown to be significant in previous studies. The bearing area of a bar per unit length is proportional to rib height (h) and inversely proportional to rib spacing (ln). This means that a bar with a large value of (h/ln) has a large bearing area. Although there is some scatter, especially for concrete strength of 120 MPa, the average bond stress and the initial stiffness tend to increase with (h/ln) up to (h/ln)=0.2, regardless of concrete strength as shown in Figures 8.4(a) and 8.4(b). The results of quadratic regression analysis for each concrete strength are also shown in Figure 8.4. For (h/ln) larger than 0.2, the bond stresses tend to be constant. On the other hand, (h/ln) has little influence on the bond stress at first splitting as shown in Figure 8.4(c).

Kokubu and Okamura conducted pullout tests of specimens with 34 MPa concrete and D51 deformed bars (51 mm diameter) using similar specimens. They reported that specimens with h/l_0 (l_0 is a clear spacing of rib) larger than 0.23 exhibited less initial bond stress [14]. The results from the tests reported here are in agreement with that observation.

(a) Average bond stress
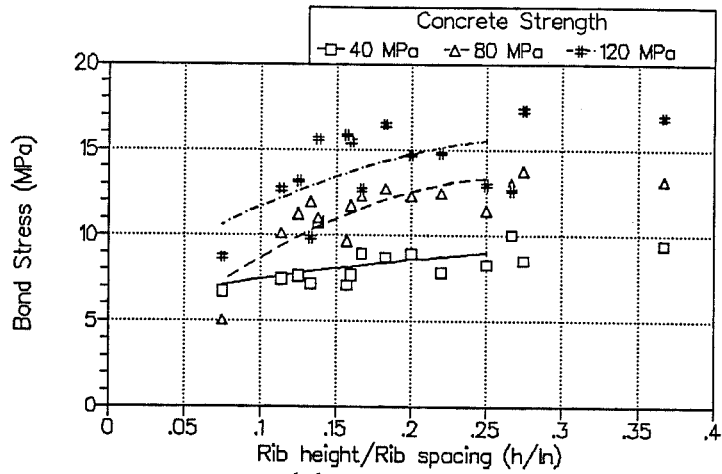
(b) Initial Stiffness
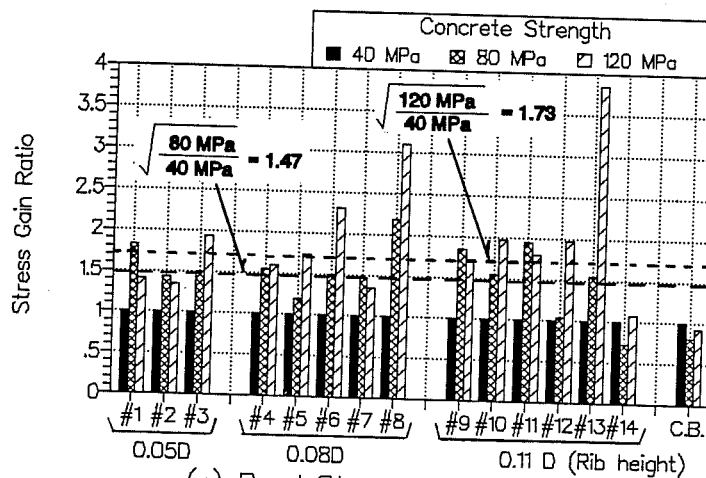
(c) Bond Stress at First Splitting

Figure 8.4 Effect of ratio of rib height to rib spacing (h/ln)
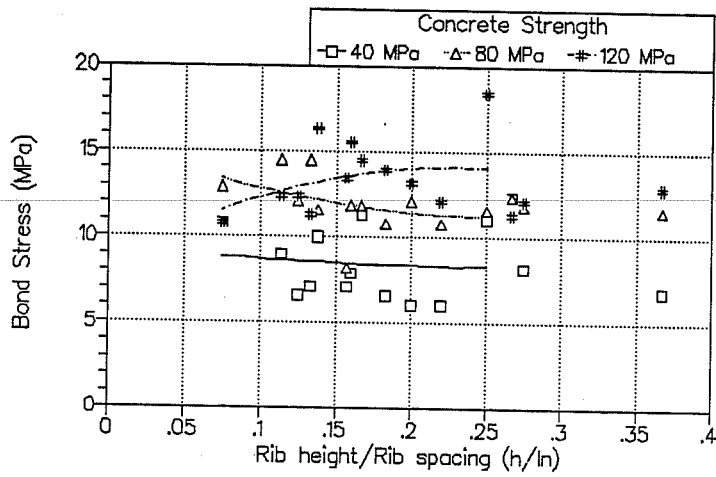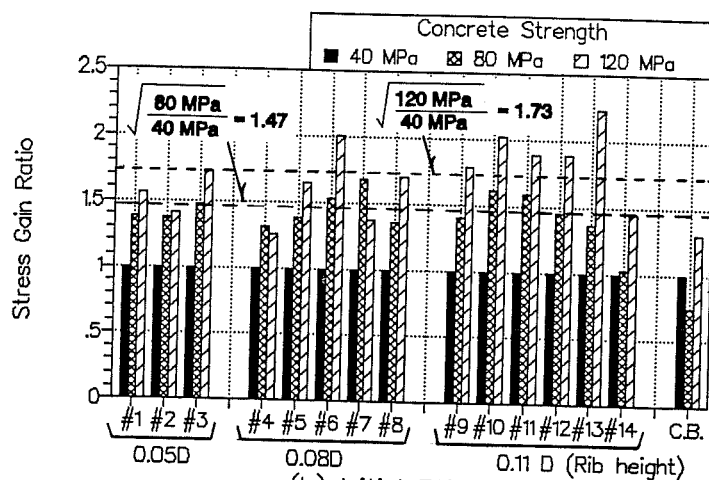
58

4) Effect of concrete strength :

The test results for specimens with the same bar deformation but different concrete strength are also compared in Figures 8.2, 8.3 and 8.4. The strength ratios for relative to the 40 MPa test specimens with the same bar deformation are given in Table 8.2 and compared in Figure 8.5. The average ratios for the average bond stress, the initial stiffness and the bond stresses at first splitting are given in Table 8.2. The measured compressive strengths of the concrete were 38.3, 82.9 and 115.1 MPa. The square roots of the measured concrete strength give ratios of 1.47 and 1.73 for 80/40 MPa and 120/40 MPa specimens. It can be concluded that for the indices used to evaluate bond performance in this paper, the square root of the concrete strength represents the trends in the data quite well.

Table 8.2 Effect of concrete strength

Bar Number	Average Bond Stress (Ratio)		Initial Stiffness (Ratio)		at First Split (Ratio)	
	$\frac{80 \text{ MPa}}{40 \text{ MPa}}$	$\frac{120 \text{ MPa}}{40 \text{ MPa}}$	$\frac{80 \text{ MPa}}{40 \text{ MPa}}$	$\frac{120 \text{ MPa}}{40 \text{ MPa}}$	$\frac{80 \text{ MPa}}{40 \text{ MPa}}$	$\frac{120 \text{ MPa}}{40 \text{ MPa}}$
#1	1.38	1.56	1.82	1.41	1.05	1.67
#2	1.38	1.41	1.43	1.33	1.05	1.28
#3	1.48	1.73	1.50	1.93	1.84	1.88
#4	1.30	1.26	1.54	1.58	1.00	.91
#5	1.38	1.64	1.18	1.73	2.00	2.17
#6	1.53	2.01	1.50	2.31	1.50	1.97
#7	1.67	1.38	1.47	1.33	2.04	1.59
#8	1.36	1.70	2.18	3.09	1.62	1.38
#9	1.40	1.79	1.83	1.71	1.69	1.88
#10	1.61	2.02	1.54	1.96	1.45	1.48
#11	1.59	1.89	1.95	1.79	1.78	2.00
#12	1.45	1.88	1.04	1.96	1.64	2.12
#13	1.36	2.23	1.54	3.85	1.15	1.89
#14	1.02	1.45	.72	1.08	1.16	1.63
Com.Bar	.75	1.30	.81	.93	1.20	1.00
Average	1.38	1.68	1.47	1.87	1.48	1.66
$\sqrt{\dfrac{\text{Meas.fc'}}{38.3}}$	1.47	1.73	1.47	1.74	1.47	1.73

59

Figure 8.5 Effect of concrete strength

8.2 Relation between bearing stress and bar deformation geometry

Because bearing area was shown to be an important factor influencing the bond performance, the results were evaluated using bearing stress rather than bond stress. Vertical axis of Figure 8.1 is changed to "Bearing Stress", the initial stiffness, average stress and first splitting are determined in terms of bearing area. Table 8.3 lists the results in terms of bearing stress.

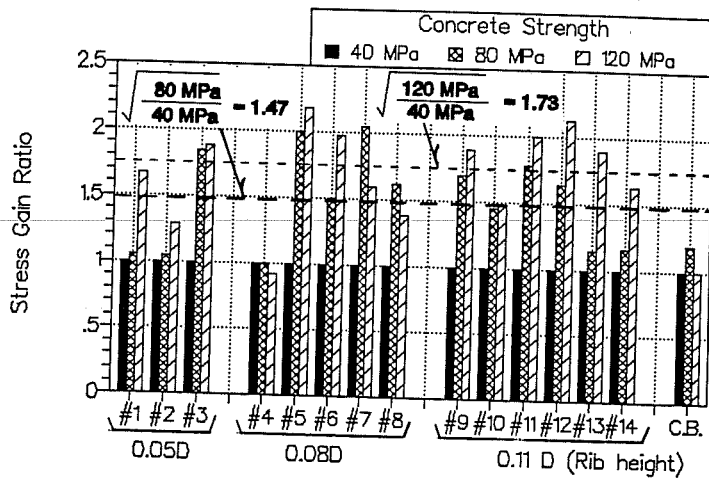Bearing stress (σ_r) is the pullout load divided by total projected area of rib faces.

$$\sigma_r = P / ((d+h) \pi h n) \qquad \cdots \cdots \cdots \cdots (2)$$

where P is a load, d is the minimum bar diameter(see Table 5.2), h is the rib height and n is the number of ribs in the anchored length. Eq.(3) is obtained by substituting $d+h$ for D and n for ($1/ln$) in Eq.(2).

$$\sigma_r = P / ((\pi D l) \cdot (h/ln))$$
$$= \tau / (h/ln) \qquad \cdots \cdots \cdots \cdots (3)$$

Table 8.3 Test results in terms of bearing stresses

Bar Number	Average Bearing Stress (MPa)			Initial Stiffness (MPa)			Bearing Stress at First Splitting (MPa)		
	Concrete Strength			Concrete Strength			Concrete Strength		
	40 MPa	80 MPa	120 MPa	40 MPa	80 MPa	120 MPa	40 MPa	80 MPa	120 MPa
#1	33.25	45.87	51.78	17.87	32.59	25.23	44.16	46.26	73.60
#2	52.96	72.83	74.81	32.66	46.66	43.55	66.88	69.99	85.55
#3	62.72	92.56	108.23	30.28	45.41	58.39	54.06	99.48	101.64
#4	37.47	48.82	47.15	23.59	36.37	37.35	46.19	46.19	42.26
#5	46.43	63.89	76.26	30.07	35.53	51.93	31.43	62.87	68.33
#6	49.27	75.24	98.91	26.96	40.44	62.35	50.55	75.83	99.42
#7	61.28	102.30	84.31	33.70	49.43	44.93	60.66	123.57	96.61
#8	75.86	103.11	129.22	29.46	64.28	91.06	91.06	147.30	125.87
#9	24.21	33.96	43.33	16.22	29.73	27.71	17.57	29.73	33.11
#10	30.12	48.59	60.93	22.24	34.29	43.56	28.73	41.70	42.63
#11	34.07	54.10	64.29	21.72	42.29	38.86	26.29	46.86	52.58
#12	50.32	73.06	94.63	36.34	37.85	71.16	37.85	62.08	80.25
#13	48.77	66.46	108.56	23.46	36.09	90.23	48.73	55.94	92.04
#14	73.42	74.95	106.46	44.83	32.27	48.41	68.13	78.89	111.17
Com.Bar	94.10	70.55	122.16	51.51	41.58	47.83	150.86	180.29	150.86

61

Therefore, bond stress (τ) and bearing stress (σ_r) are a function of (h/ln) in the following manner.

$$\tau = \sigma_r \cdot (h/ln) \qquad\qquad \cdots\cdots\cdots (4)$$

1) Effect of rib spacing :

Figure 8.6 shows the effect of rib spacing on bearing stress grouping the bars with the same rib height together. The average bearing stress and bearing stress at first splitting increased as rib spacing increased for all concrete strength. The relation between initial bearing stress and rib spacing generally shows the same trend although the results showed more variation.
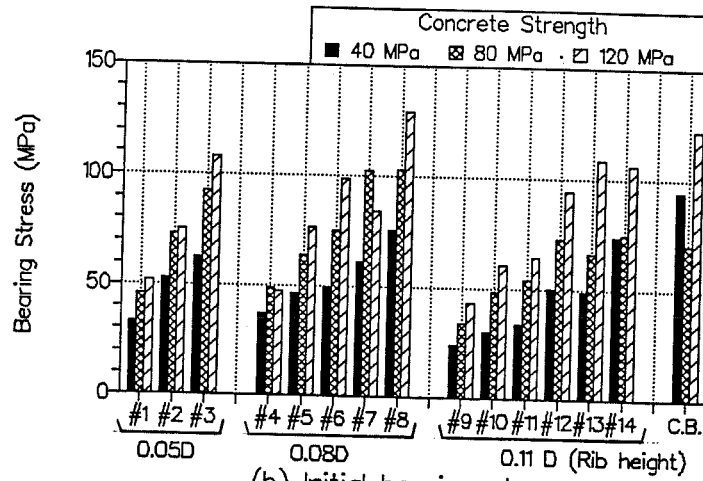
2) Effect of rib height :

Bars with the same rib spacing are grouped in Figure 8.7. As the test numbers increase, the rib height increases. The average bearing stress, initial bearing stress and the bearing stress at first splitting decreased as the rib height increased.

3) Effect of ratio of rib height to rib spacing (h/ln) :

Figure 8.8 shows the relationships between bearing stresses and (h/ln). Quadratic regression curves for each concrete strength are also shown in Figure 8.8. The average bearing stress, initial bearing stress and bearing stress at first splitting decreased as (h/ln) increased, regardless of concrete strength. If the relation is expressed as a hyperbolic function of $\sigma_r = a / (h/ln) + b$, where a and b are constants. The bond stress (τ) is given by $\tau = a + b \cdot (h/ln)$ where $\tau = \sigma_r \cdot (h/ln)$ is substituted into the equation. Curves for bond stress versus (h/ln) were plotted in Figure 8.4 and are of the same form as the equation derived here. However, it is difficult to determine exact values of a and b because of the data scatter.

62
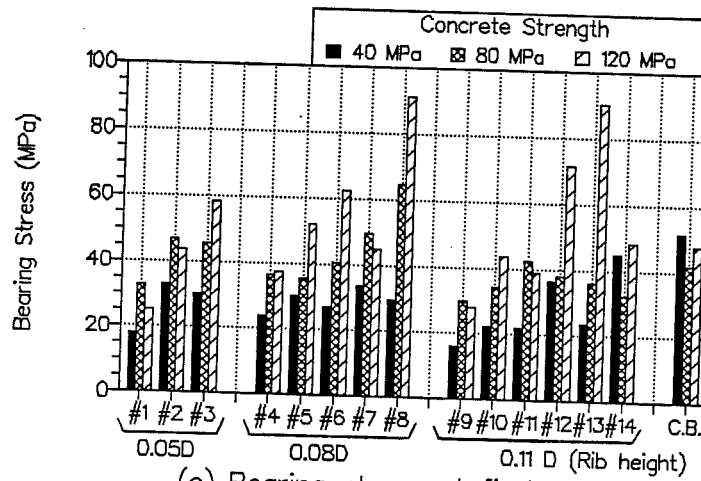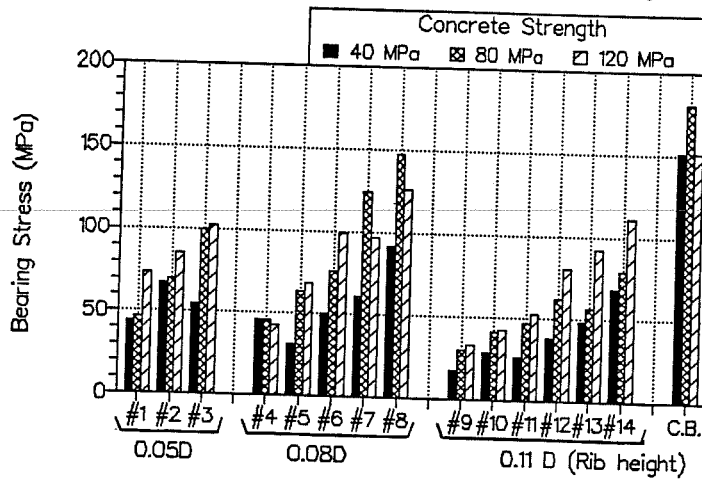
Figure 8.6 Effect of rib spacing
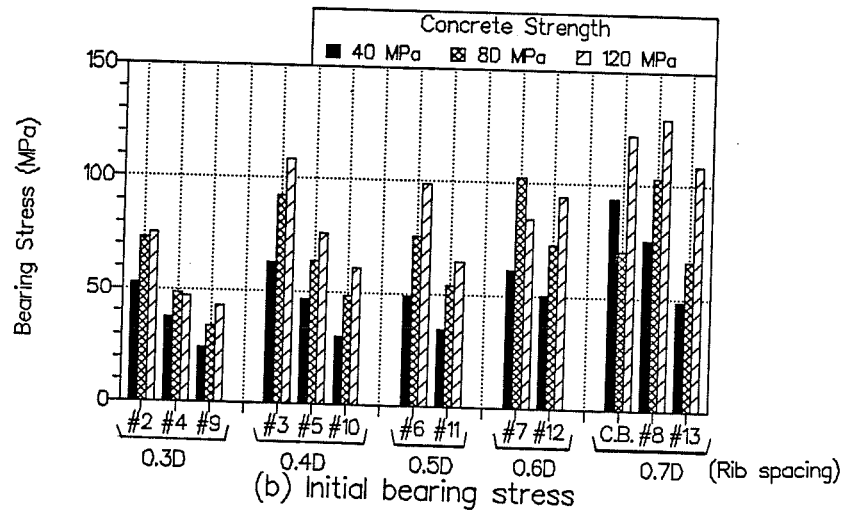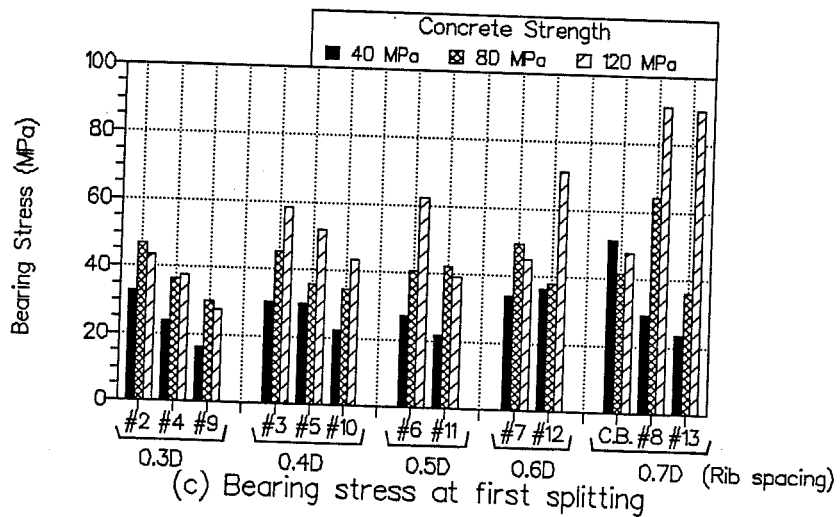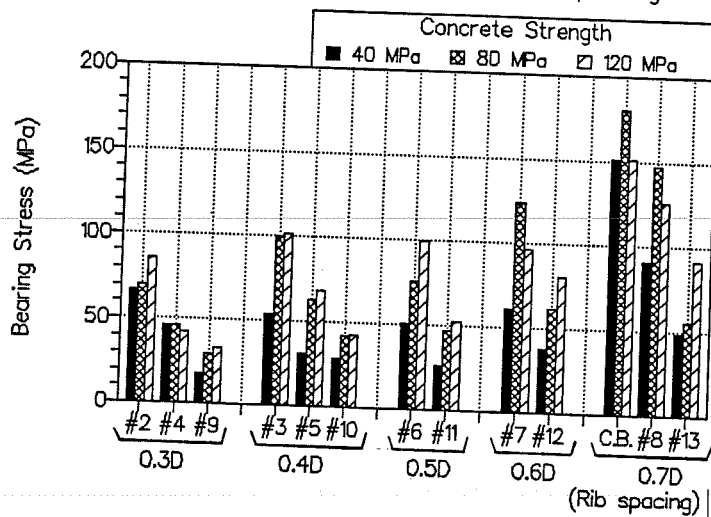
Figure 8.7 Effect of rib height
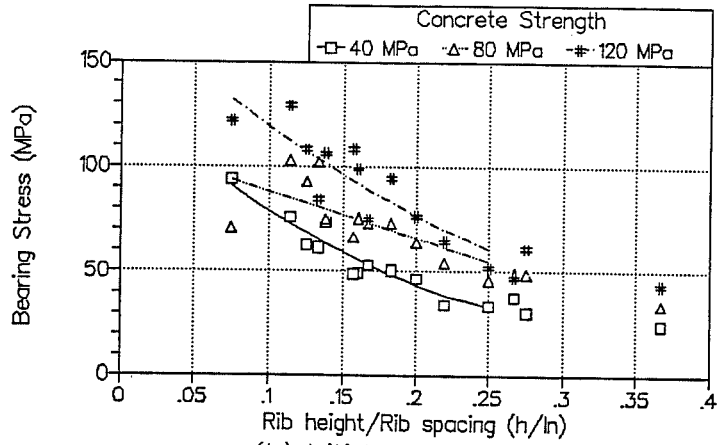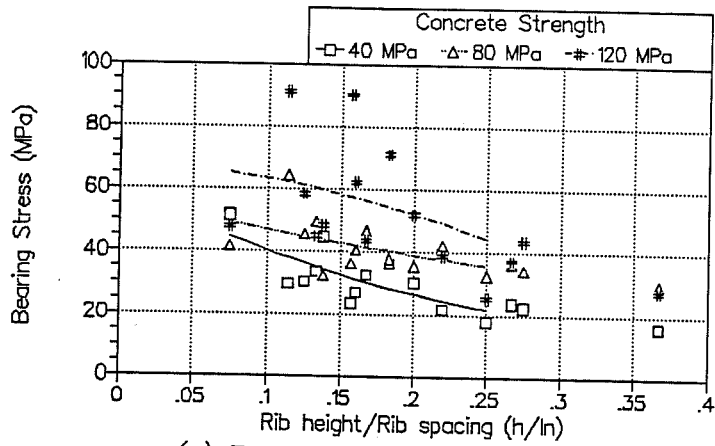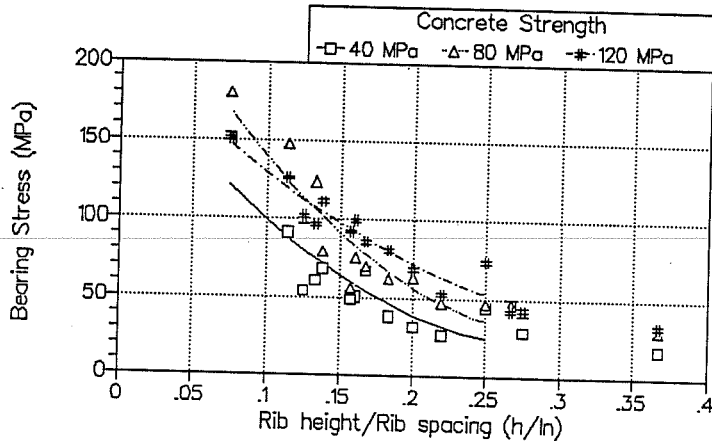
Figure 8.8 Effect of ratio of rib height to rib spacing (h/ln)

65

8.3 Relation between shear stress and bar deformation

The data could also be evaluated using average shear stress (τ_s) which is given as the pullout load divided by the shear area of rib fillet concrete.

$$\tau_s = P / ((d + 2h) \pi (1 - nw)) \quad \cdots \cdots (5)$$

where P = a load, d = the minimum bar diameter (see Table 5.2), h = the rib height, l = the bond length, n = number of ribs in bond length and w is the width of rib top. Equation (5) has the same form as Eq. (1) except that the width of the rib top surfaces are subtracted from the anchorage length. Table 8.4 lists the test results in terms of shear stress. Since this is a relatively small and systematic adjustment the results are nearly identical to those shown in Figures 8.2, 8.3 and 8.4.

Table 8.4 Test results in terms of shear stresses

| Bar Number	Average Shear Stress (MPa)			Initial Stiffness (MPa)			Shear at First Split (MPa)		
	Concrete Strength			Concrete Strength			Concrete Strength		
	40 MPa	80 MPa	120 MPa	40 MPa	80 MPa	120 MPa	40 MPa	80 MPa	120 MPa
#1	10.56	14.57	16.45	5.68	10.35	8.02	14.03	14.70	23.38
#2	10.10	13.89	14.27	6.23	8.90	8.31	12.75	13.35	16.31
#3	8.55	12.61	14.75	4.13	6.19	7.96	7.37	13.56	13.85
#4	10.95	14.26	13.77	6.89	10.62	10.91	13.49	13.49	12.35
#5	9.82	13.51	16.12	6.36	7.51	10.98	6.65	13.29	14.45
#6	7.88	12.04	15.83	4.31	6.47	9.98	8.09	12.13	15.91
#7	8.04	13.43	11.07	4.42	6.49	5.90	7.96	16.22	12.68
#8	8.45	11.48	14.39	3.28	7.16	10.14	10.14	16.40	14.02
#9	9.97	13.98	17.84	6.68	12.24	11.41	7.23	12.24	13.63
#10	8.88	14.32	17.96	6.55	10.11	12.84	8.47	12.29	12.56
#11	7.70	12.22	14.53	4.91	9.55	8.78	5.94	10.59	11.88
#12	9.33	13.55	17.55	6.74	7.02	13.20	7.02	11.51	14.88
#13	7.68	10.46	17.08	3.69	5.68	14.20	7.67	8.80	14.48
#14	10.03	10.24	14.55	6.13	4.41	6.62	9.31	10.78	15.19
Com.Bar	7.22	6.04	10.45	3.95	3.56	4.09	11.57	15.42	12.90

CHAPTER 9

Conclusions

To study the effect of deformed bar geometries and concrete strength on bond of reinforcing steel to surrounding concrete, pullout tests in which the main variables were rib height and rib spacing were conducted. Concrete strength up to 120 MPa was used. The following conclusions were made.

1) The average bond stress and the initial stiffness of the bond-slip curve increased as rib spacing decreased for concrete strengths of 40 and 80 MPa. However, no clear trend was observed for 120 MPa concrete.

2) The average bond stress and the initial stiffness of the bond stress-slip curve increased as rib height increased. The increase was larger for higher strength concrete.

3) The rib spacing or rib height did not have a significant influence on the bond stress at first splitting, regardless of concrete strength.

4) As the ratio of rib height to rib spacing (h/ln) increased, which is the same as increase in the bearing area, the average bond stress and the initial stiffness increased regardless of concrete strength. However, for (h/ln) larger than 0.2, these values seemed to be constant.

5) The trends in the observed response, as concrete strength increased, could be represented well by using ratios of the square root of the concrete strength.

6) Bars with rib face angles equal to or greater than 45 degrees exhibited almost the same bond behavior. However, bars with a rib face angle of 30 degrees were less stiff initially.

7) Machined bars with bar geometries identical to a commercial bar exhibited substantially the same load-slip response as that of the rolled commercial bar.

8) The rolled commercial bar exhibited the lowest average bond stress and initial stiffness but reasonably good bond stress at first splitting regardless of concrete strength.

APPENDIX

Behavior of 120 MPa specimens at a large slip

1) Bond - Slip Curves for a large slip

Bond characteristics up to 0.25 mm slip was discussed in this report. However, the specimens with concrete strength of 120 MPa were loaded after spalling of the cover concrete outside of the spiral hoop. The load increased again for a larger slip. Before reaching the maximum strength, some load drops and recoveries were observed. These resulted in discontinuity points in the original bond - slip curves. Correction of the bond - slip curves were made. Figures A1 and A2 show bond - slip curves of specimens with 120 MPa concrete after the correction. For most of the specimens, the maximum strength occurred at a slip less than 0.6 mm. Failure mode for all the specimens with 120 MPa concrete was shear failure of the concrete keys between ribs as shown in Figures A3, A4 and A5. The shear failure occurred after development of cracks with angles of 45 to 60 degrees to bar axis and starting from the top rib as shown in Figure A4.

2) Effect of bar deformation on the maximum strength

Table A1 lists the results at maximum strength for the specimens with 120 MPa concrete. The absolute values at maximum strength are not useful because the values must be governed by confinement of surrounding concrete of the bar. The effects of rib height, rib spacing and the ratio of rib height to rib spacing (h/ln) on the maximum bond stress are shown in Figure A6, A7 and A8, respectively. The maximum bond stress increased linearly as the rib height increased. The effect of rib height is significant however those of rib spacing and (h/ln) are not clear.
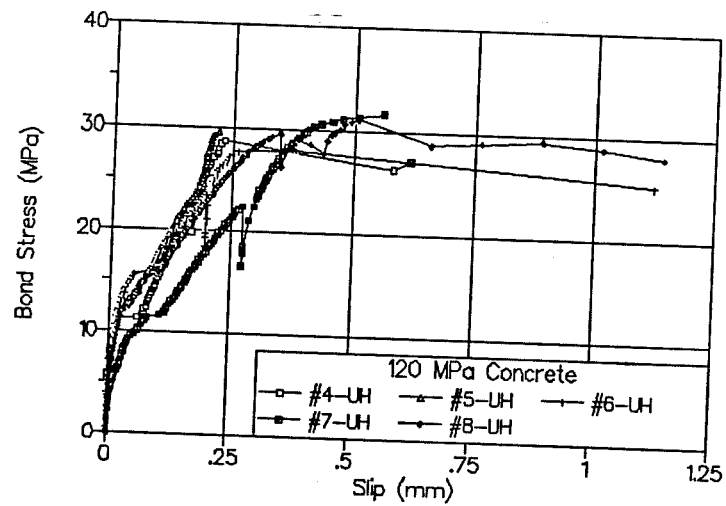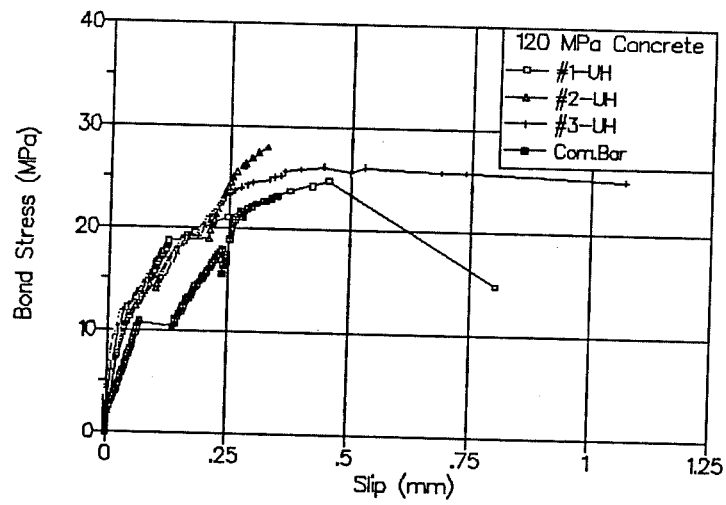
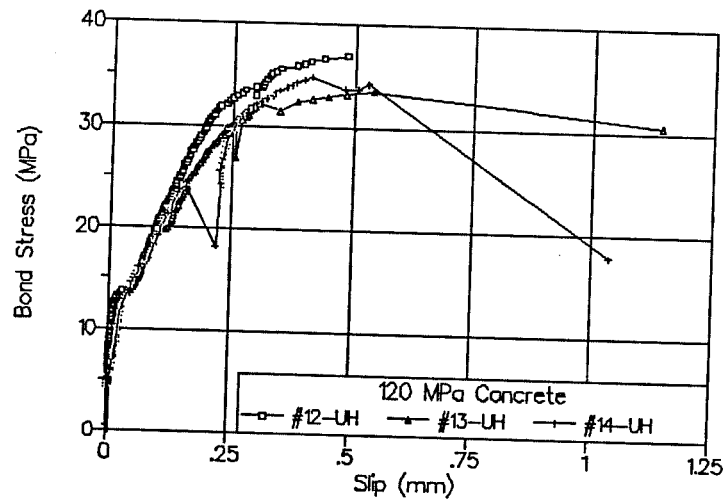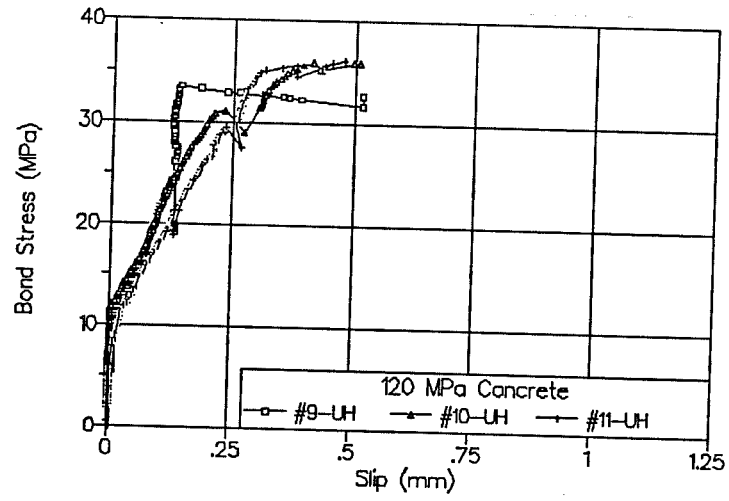Figure A1   Bond - slip curves of 120 MPa concrete specimens

Figure A2 Bond – slip curves of 120 MPa concrete specimens

Table A1   Results at maximum strength

Specimen	at Maximum Strength			
	Bond Stress (MPa)	Bearing Stress (MPa)	Shear Stress (MPa)	Slip (mm)
#1-UH	24.8	98.8	31.4	0.452
#2-UH	27.9	164.9	31.4	0.325
#3-UH	26.1	214.1	29.2	0.442
#4-UH	28.7	107.1	31.3	0.231
#5-UH	29.5	153.1	32.4	0.218
#6-UH	27.9	178.6	28.6	0.378
#7-UH	31.6	269.6	35.4	0.559
#8-UH	31.1	316.0	35.2	0.505
#9-UH	33.5	85.8	35.3	0.140
#10-UH	35.8	126.0	37.1	0.411
#11-UH	35.6	154.3	34.9	0.475
#12-UH	36.9	212.0	39.3	0.483
#13-UH	33.5	229.2	36.1	0.538
#14-UH	34.8	236.7	32.3	0.409
Com.Bar	27.7	386.3	33.9	2.430

Figure A3   Final appearance of "#1-UH"
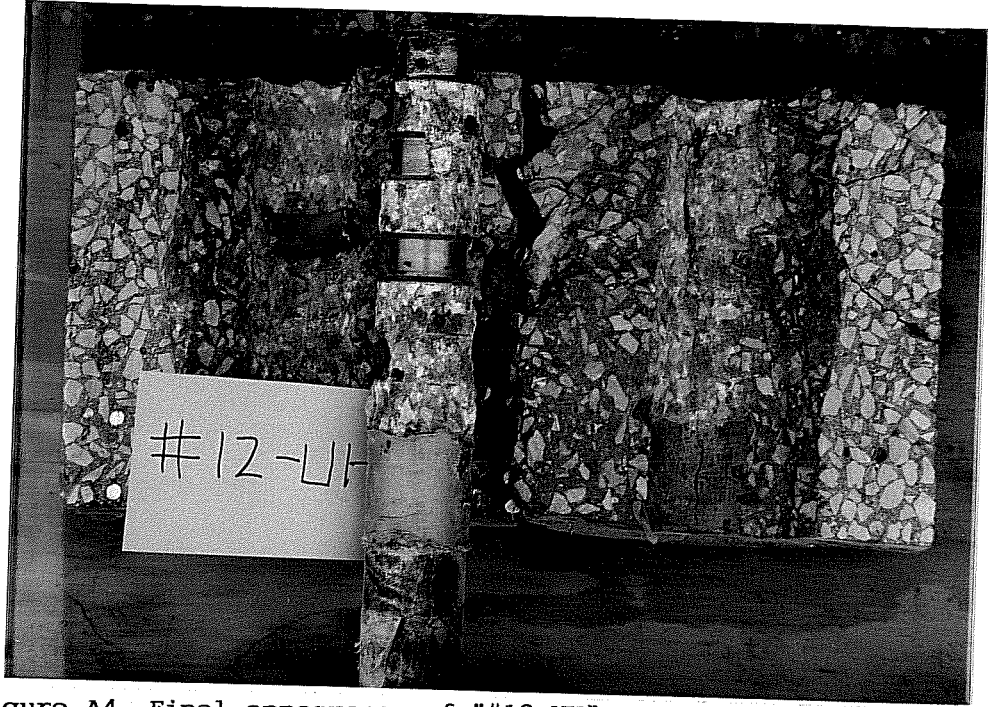(Concrete keys were sheared off)

Figure A4 Final appearance of "#12-UH"
(Shear failure occurred after cracks with angles of
45° to 60° to bar axis)

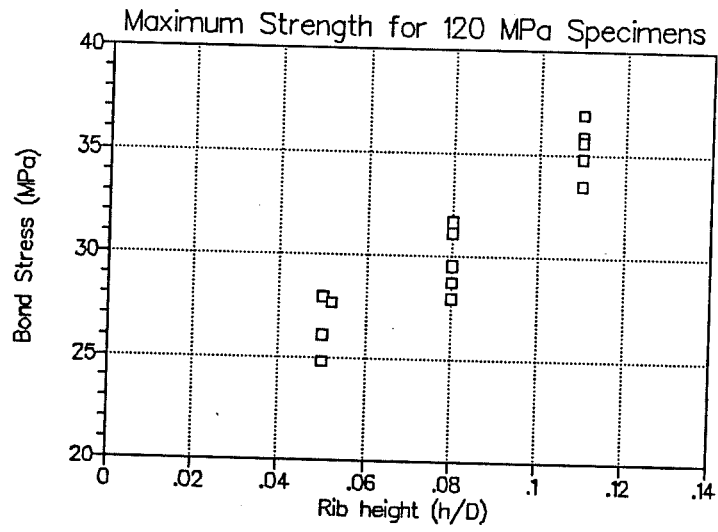

Figure A5 Close-up of concrete keys sheared off
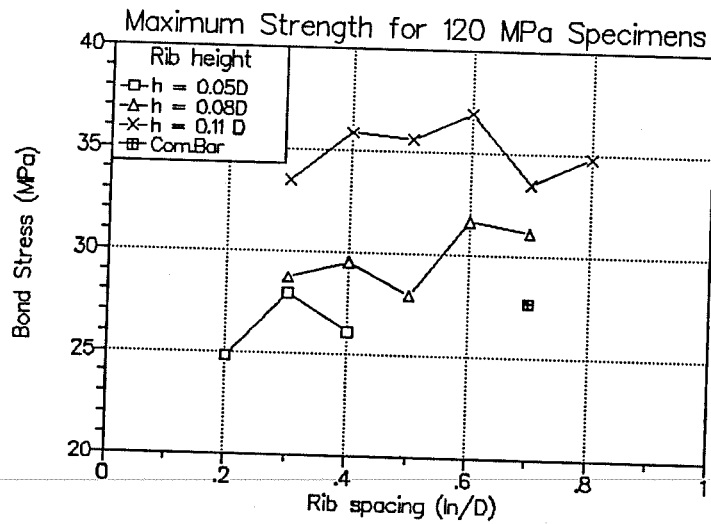
Figure A6   Effect of rib height

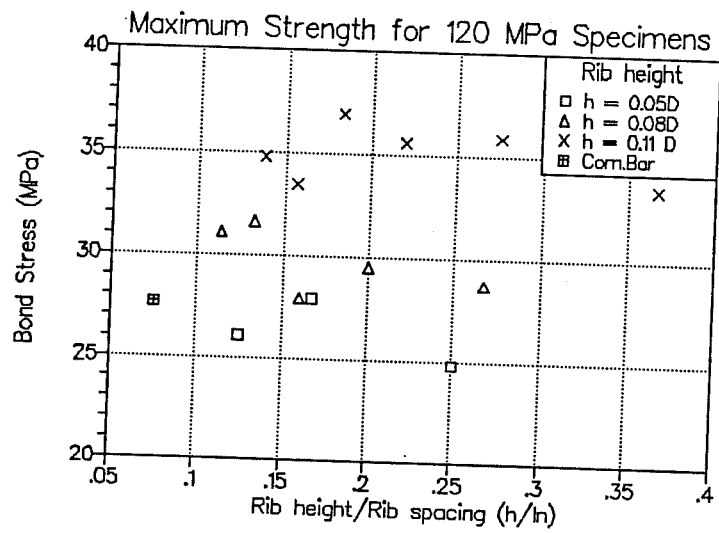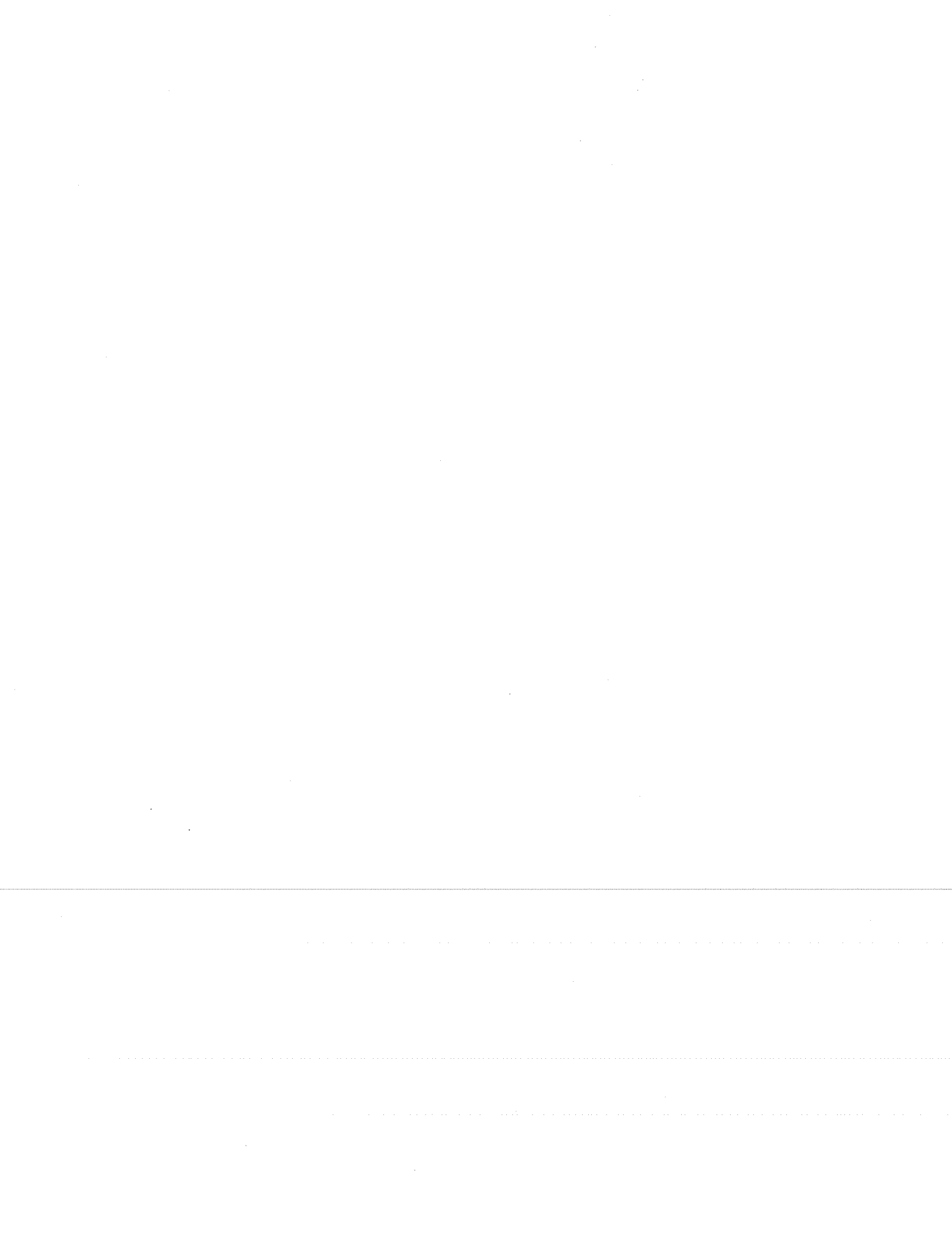Figure A7   Effect of rib spacing

74

Figure A8   Effect of (h/ln)

REFERENCES

[1] Abrams, D. A., "Tests of Bond Between Concrete and Steel," Bulletin No.71, University of Illinois Engineering Experiment Station, Urbana, 1913.

[2] Menzel, C. A., "Some Factors Influencing Results of Pull-Out Bond Tests," ACI Journal, Proceedings V.35, June 1939, pp.517-544.

[3] Clark, A. P., "Comparative Bond Efficiency of Deformed Concrete Reinforcing Bars," ACI Journal, Proceedings V.18, No.4, December 1946.

[4] Clark, A. P., "Bond of Concrete Reinforcing Bars," ACI Journal, Proceedings V.46, October 1949, pp.161-184.

[5] Rehm, G., "The Fundamental Law of Bond," RILEM-Symposium on Bond and Crack Formation in Reinforced Concrete, Stockholm, V.2, 1957, pp. 491-498.

[6] Shah, I. K., "Behavior of Bond Under Dynamic Loading," Research Report R63-17, School of Enginering, Massachusetts Institute of Technology, Cambridge, March 1963.

[7] Ferguson, P. M., Breen, J. E., and Thompson, J. N.,"Pullout Tests on High Strength Reinfoecing Bars," ACI Journal, Proceedings V.62, No.8, August 1965, pp.933-950.

[8] Lutz, L. A., and Gergely, P., "The Mechanics of Bond and Slip of Deformed Bars in Concrete," ACI Journal, Proceedings V.64, No.11, November 1967, pp.711-721.

[9] Wilhelm, W. J., Kemp, E. L., and Lee, Y. t., "Influence of Deformation Height and Spacing on The Bond Characteristics of Steel Reinforcing Bars," Civil Engineering Studies Report No.2013, Department of West Virginia University, 1971.

[10] Skorobogatov, S. M., and Edwards, A. D., "The influence of the Geometry of Deformed Steel Bars on Their Bond Strength in Concrete," Proceedings Instn. Civ. Engrs, Part 2, V.67, June 1979, pp.327-339.

[11] Losberg, A., and Olsson, P. A., "Bond Failure of Deformed Reinforcing Bars Based on The Longitudinal Splitting Effect of The Bars," ACI Journal, Proceedings V.76, No.1, January 1979, pp.5-18.

[12] Soretz, S. and Hölzenbein, H.,"Influence of Rib Dimensions of Reinforcing Bars on Bond and Bendability," ACI Journal, Proceedings V.76, No.1, Jan. 1979, pp.111-125

[13] Murata,J. and Kawai,A., "Studies on Bond Strength of Deformed Bar by Pull-Out Test", journal of Japanese Society of Civil Engineering, No.348/v-1, August 1984, pp.113-122.(in Japanese)

[14] Kokubu, M. and Okamura, H., "Studies on Usage of Large Deformed Bar",Concrete Library No.43, Japanese Society of Civil Engineering, August 1977, pp.19-29 (in Japanese)

[15] Goto,Y.,Shima,H. and Otsuka,K.,"Studies on Bond Characteristics of Large Deformed Bar",Concrete Library, No.43, Japanese Society of Civil Engineering, August 1977, pp.43-54 (in Japanese)

[16] Akasi,J., Fujii,S. and Morita,S.,"Effect of Concrete Strength and Bar Deformation on Bond Behavior", Proceedings of the Japan Concrete Institute, Vol.13, 1991. (in Japanese)